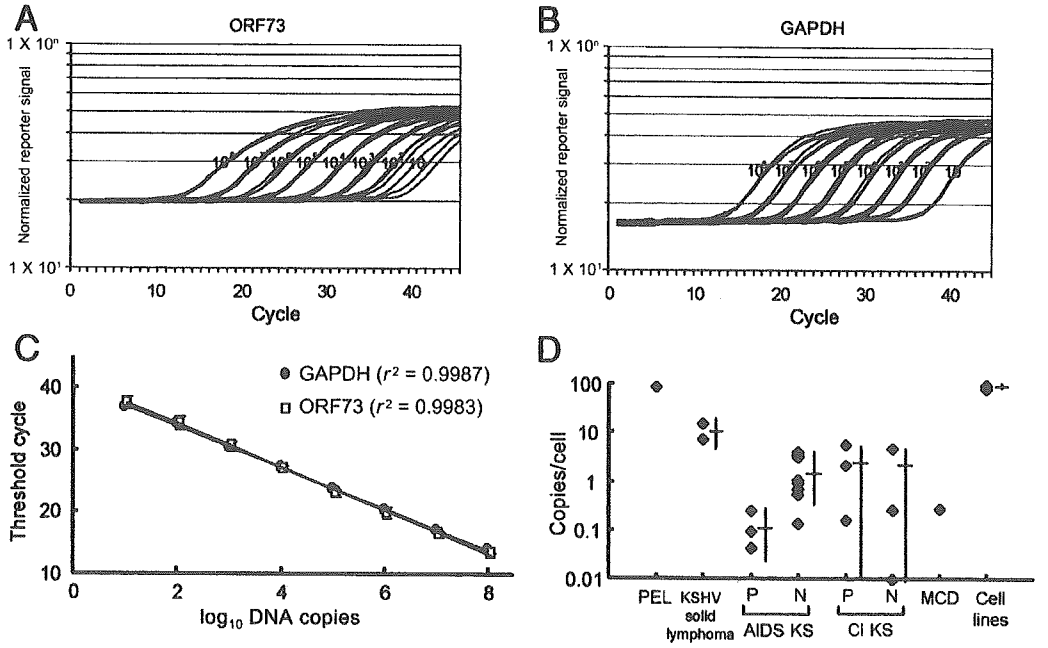

Figure 1. No. of copies of Kaposi sarcoma–associated herpesvirus (KSHV) in KSHV-associated diseases, determined by real-time polymerase chain reaction (PCR). *A* and *B*, Amplification curves of open-reading frame (ORF)–73 *(A)* and glyceraldehyde 3-phosphate dehydrogenase (GAPDH) genomes *(B)*. *C*, Standard curve of ORF73 and GAPDH genomes. *D*, No. of copies of KSHV per cell, calculated on the basis of the results of real-time PCR. Horizontal and vertical bars beside blots indicate average and SD, respectively. AIDS KS, AIDS-associated KS; Cl KS, classic KS; MCD, multicentric Castleman disease; N, nodular; P, patch; PEL, primary effusion lymphoma; Rn, normalized reporter signal.

Computerized-image analysis for KSHV-positive cells. To estimate numbers of KSHV-infected cells in lesions of KSHV-associated diseases, computerized analysis of immunohistochemical images was performed using ImageJ software (version 1.33u; National Institutes of Health). A representative image of each section from each sample was captured at ×40 or ×100 magnification. First, the image was split into red, green, and blue colors; then the 3 images were converted to gray-scale images. The total number of cells was counted in the red image, and the number of KSHV-infected cells (stained by the antiserum against KSHV proteins) was counted in the blue image. A threshold was set, for clear visualization of the displayed image. For counting cells, "analyze particle" was selected from "analyze" in the menu bar, and the minimum size was set at 30. After the accuracy of cell outlines generated by the software was verified, numbers of cells were calculated in separate windows.

RESULTS

Amount of KSHV viral genome in KSHV-associated lesions. To determine the relationships between amounts of KSHV genome and KSHV-associated diseases, we performed real-time PCR to detect KSHV ORF73 and GAPDH in appropriate DNA samples. Specificity of the assay for ORF73 was confirmed using a panel of DNA from other herpesviruses (HHV-1–7) and cellular DNA from HUVECs and Raji cells (data not shown). The assay for ORF73 uniformly detected 10 copies of pGEM-ORF73 plasmid (figure 1*A* and 1*C*). PCR amplification of GAPDH also uniformly detected 10 copies of GAPDH genome (figure 1*B* and 1*C*). Amplification plots and standard curves demonstrated a linear relationship between numbers of copies from 10 to 10^8 and the cycle threshold, which indicates that dynamic ranges of these 2 real-time PCRs were between 10 and 10^8 copies. To validate differences between DNA samples from frozen tissues and those from paraffin-embedded tissues, we tested a DNA sample from a frozen cell pellet of TY-1 and a DNA sample from a paraffin-embedded TY-1 cell pellet. No significant difference was detected between these 2 types of DNA (data not shown).

Results of real-time PCR showed signs of a positive association between the number of viral copies per cell and disease (table 1 and figure 1*D*). A DNA sample from PEL demonstrated a number of KSHV copies similar to that of PEL cell lines (PEL, 82; PEL cell lines, 87). DNA from samples of KSHV-associated solid lymphoma also showed a high number of KSHV copies (average, 10.8 viral copies/cell). DNA from samples of KS and MCD demonstrated lower numbers of viral copies than those of KSHV-associated lymphoma (PEL and KSHV-associated solid lymphoma). The average number of KSHV copies in DNA from KS samples was 1.58 viral copies/cell (range, 0.00–5.50

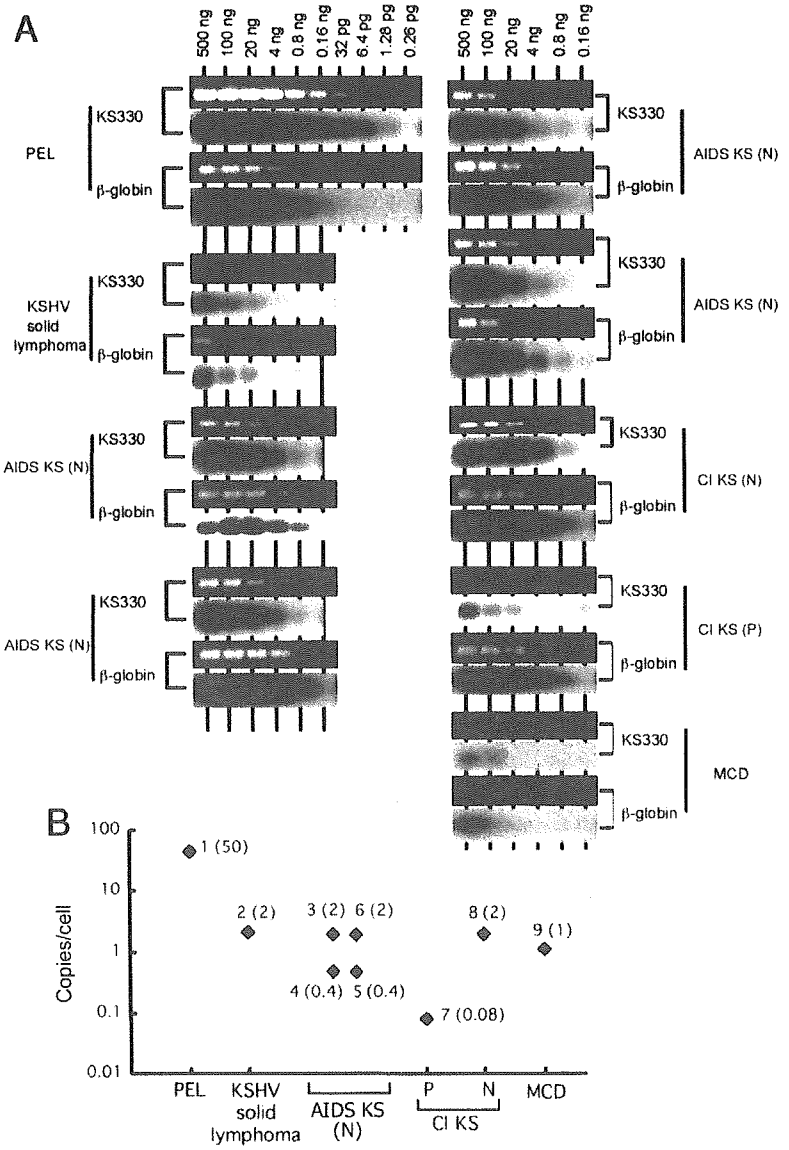

Figure 2. No. of copies of Kaposi sarcoma–associated herpesvirus (KSHV) in KSHV-associated disease, determined by conventional polymerase chain reaction (PCR)–Southern blotting. *A*, PCR–Southern blotting. DNA extracted from samples was serially diluted, and KS330 and β-globin genes were amplified from the diluted DNA. *Upper panels*, bands of PCR products in ethidium bromide–stained gel; *lower panels*, bands of products in PCR–Southern blots. *B*, No. of copies of KSHV in KSHV-associated diseases, determined by PCR–Southern blots. The nos. beside each dot correspond to the sample nos. in panel A. The nos. in parentheses indicate the nos. of viral copies per cell. AIDS KS, AIDS-associated KS; CI KS, classic KS; MCD, multicentric Castleman disease; N, nodular; P, patch.

viral copies/cell), whereas those in DNA samples from the nodular and patch/plaque stages of AIDS-associated KS samples were 1.72 and 0.13 viral copies/cell, respectively. DNA samples from classic KS (KS in patients without HIV infection) also had <5 viral copies/cell. A DNA sample from an MCD lesion had 0.27 viral copies/cell. To confirm these results, we performed semiquantitative PCR–Southern blot analysis using some of these samples. Results demonstrated similar copy numbers resulting from the 2 techniques (table 1 and figure 2). Thus, quantitative PCR analysis suggested that PEL might have the highest copy number (82 copies), followed by KSHV-associated solid lymphoma (11 copies). KS and MCD lesions contained lower copy numbers (~1 copy/cell), regardless of HIV-infection.

Number of KSHV-infected cells in KSHV-associated diseases. Because pathologic tissue samples present cells contaminated

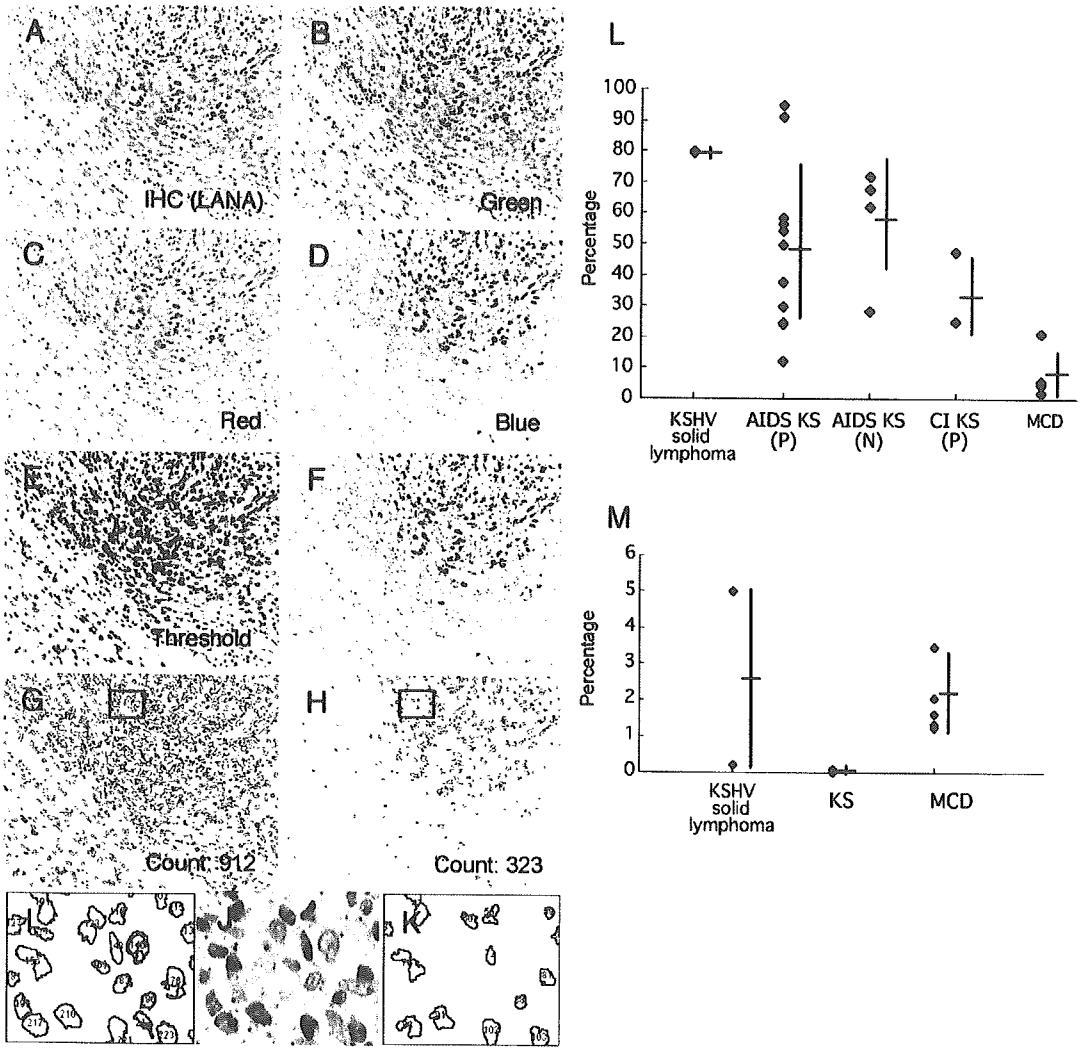

Figure 3. Computerized-image analysis of immunostaining. *A–K,* Samples of computerized-image analysis. *A,* Image of immunohistochemical analysis for latency-associated nuclear antigen (LANA) on the lymph node that Kaposi sarcoma (KS) cells infiltrate. *B–D,* Image separated in into red *(C),* green *(B),* and blue *(D)* splits. *E,* The threshold of all cells, determined on the basis of a red split. *F,* The threshold of positive cells, determined on the basis of a blue split. *G,* Tracing image of all cells. *H,* Tracing image of only positive cells. *I,* Enlarged image of a box from panel I. All cells were traced and counted. *J,* The image of immunohistochemical analysis corresponding to that in panel I. *K,* Enlarged image of a box in panel H. Only positive cells were traced and counted. *L,* Rate of LANA-positive cells in samples. Horizontal and vertical bars beside blots indicate the average and SD, respectively. *M,* Positive rate of open-reading frame (ORF)–50–positive cells. AIDS KS, AIDS-associated KS; CI KS, classic KS; KSHV, KS-associated herpesvirus; MCD, multicentric Castleman disease; N, nodular; P, patchy.

in varying degrees, all DNA samples that we used for real-time PCR actually contained DNA extracted from histologically normal cells and noninfected (LANA-negative) cells, as confirmed by histologic data. To determine accurate KSHV copy numbers in a KSHV-infected cell in a lesion, knowledge is required of accurate numbers of KSHV-infected cells in a specific sample. Thus, we performed computerized-image analysis of immunostained sections to estimate the number of KSHV-positive cells. Because it is recognized that all KSHV-infected cells express LANA in the nuclei, we counted cells expressing LANA in the nuclei as KSHV-infected cells. LANA was stained brown in immunohistochemical analysis, and cell nuclei were counterstained with hematoxylin (violet). Therefore, brown nuclei were counted as LANA-positive cells, and violet entities were counted as nuclei by the image-analysis software ImageJ (figure 3). Results revealed that 80% of cells in tissue samples from KSHV-associated solid lymphoma were LANA positive (table 2 and figure 3*L*). Tissues obtained from AIDS-associated and non–AIDS-associated KS contained 12%–95% (average, 49%) LANA-positive cells. The MCD sample contained 8% (range,

Table 3. No. of viral copies and percentage of latency-associated nuclear antigen (LANA–) or open-reading frame (ORF)–50–positive cells in Kaposi sarcoma–associated herpesvirus (KSHV)–associated diseases.

Samples	Detected viral copies/cell[a]	LANA positive,[b] %	ORF50 positive,[b] %	Lytic cells/ infected cells, %	Predicted viral copies/infected cell
PEL	82.01	ND	ND	ND	...
KSHV-associated solid lymphoma	10.7	80	3	4	13.4
KS	1.58	49	0	0	3.22
AIDS-associated KS	1.28	51	0	0	2.50
Patch/plaque	0.13	48	0	0	0.27
Nodular	1.72	57	0	0	3.02
Classic KS	2.12	36	0	0	5.89
MCD	0.27	8	2	25	3.38

NOTE. MCD, multicentric Castleman disease; ND, not done; PEL, primary effusion lymphoma.

[a] TaqMan polymerase chain reaction.

[b] Immunohistochemical analysis.

5%–21%) LANA-positive cells. By comparing results from quantitative PCR and computerized-image analysis, we predicted numbers of KSHV copies in virus-infected cells from KSHV-associated disease samples (table 3). The predicted number of KSHV copies was 3.2 viral copies/cell in KS lesions. We also counted cells positive for ORF50 protein, a lytic antigen encoded by KSHV (table 2 and figure 3*M*). There were 3% ORF50 protein–positive cells in KSHV solid lymphoma samples and even a smaller percentage in KS lesions (table 2 and figure 4). When we compared numbers of cells expressing ORF50 protein and those expressing LANA, it was clear that KS cells expressed LANA, but the expression of ORF50 protein was very rare in KS lesions (table 3). In MCD lesions, 2% of cells expressed ORF50 protein. Although only 8% of cells were virus infected in MCD lesions, 25% of virus-infected cells expressed ORF50 protein, which suggests the frequent lytic replication of KSHV in MCD. These data demonstrated that number of viral copies and positivity for LANA varied among KSHV-associated diseases, which suggests different mechanisms of viral pathogenesis.

Numbers of KSHV copies at each KS stage. KS lesions were categorized into 3 clinical stages: patch, plaque, and nodular. To determine the relationship between amounts of KSHV genome and KS clinical stage, amounts of viral genome and cellular gene present in DNA extracts from specimens at each KS stage were examined using quantitative real-time PCR (figure 1) and semiquantitative PCR–Southern blotting (figure 2). The number of KSHV copies was significantly lower in patch/plaque-stage lesions (range, 0.04–0.30 viral copies/cell; average, 0.13 viral copies/cell) than in nodular-stage lesions (range, 0.10–3.90 viral copies/cell; average, 1.72 viral copies/cell) ($P < .05$, Mann-Whitney U test). In contrast, the number of KSHV copies was similar in both patch/plaque- and nodular-stage lesions in classic KS. Computerized-image analysis of immunohistochemically stained sections revealed that LANA-positive cell populations in the nodular stage (57%) were larger than those in the patch/plaque stage (48%); however, there was no significant difference between them. Lytic ORF50 protein–positive cells were very rare (0%) in both stages (figure 3*L* and 3*M* and table 3), which implies that lesions in KS were mainly composed of proliferating KSHV latently infected cells. Differences in numbers of viral copies between the 2 stages in AIDS-associated KS may simply be related to the numbers of latently infected cells.

KSHV-positive cells during the early stage of KS. According to the results of quantitative PCR, relatively high numbers of KSHV copies were detected in patch-stage KS tissue samples (figure 1*D*). In addition, KSHV-positive cells were detected at a rate of ~50% even during the early stage of KS, although numbers of viral copies in DNA from patch-stage samples were lower than those in nodular-stage samples. To clarify why such a high number of viral copies was present during the patch stage of KS, we investigated the localization of KSHV-positive cells in histologically stained sections at the patch stage. Histologic analysis showed an abnormal enlargement of blood capillaries with extended endothelial cells during the patch stage (figure 4*A*). Spindle cells were also sometimes observed around vessels at this stage. Many previous research groups have reported that these spindle-shaped cells were positive for KSHV; however, there has been no report that has described the KSHV status of these extended endothelial cells in enlarged capillaries during the early stage of KS. Here, double labeling revealed that both enlarged endothelial cells and spindle cells around capillaries were positive for LANA and VEGFR-3 (figure 4*A* and 4*B*). VEGFR-3 is a marker of lymphatic endothelial cells, and it is known that KSHV infection alters the gene profile and induces the expression of VEGFR-3 in endothelial cells [31–33]. All KS spindle cells at every stage expressed both LANA and VEGFR-3 (figure 4*A*–4*F*). No signal for LANA or VEGFR-3 was found in normal endothelial cells from capillaries or blood vessels in KS lesions (figure 4*C* and 4*D*). These data suggest that KSHV may infect endothelial cells at a very early

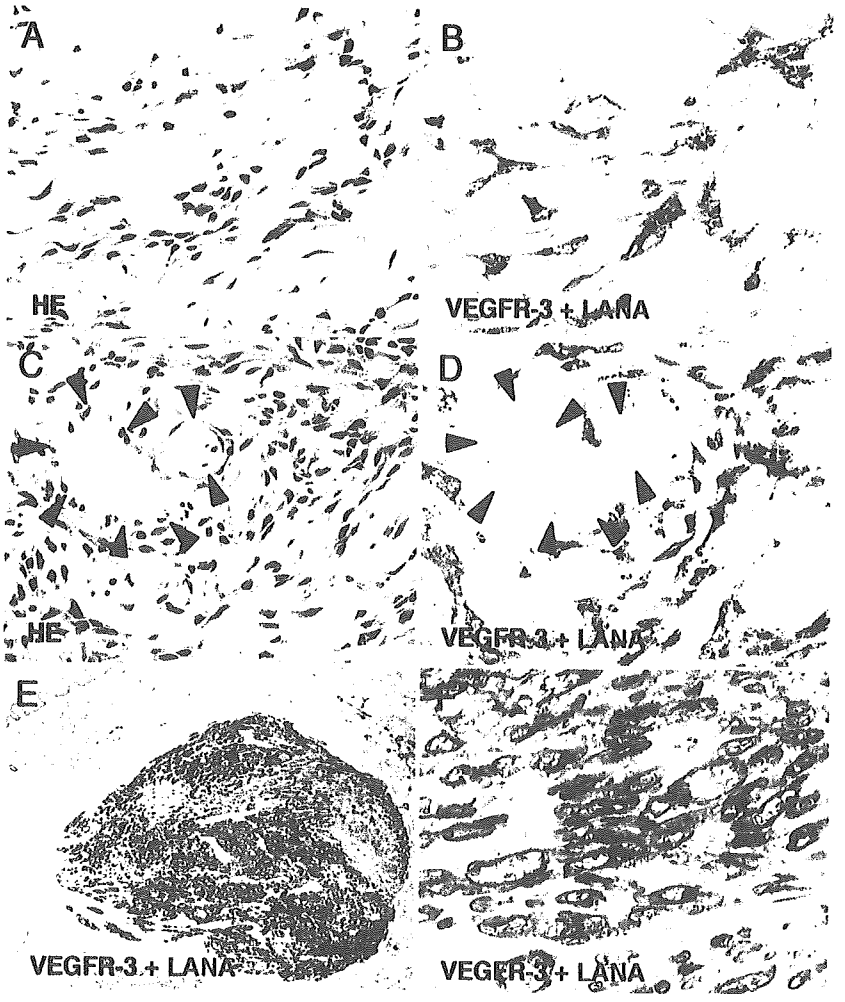

Figure 4. Kaposi sarcoma (KS)–associated herpesvirus–positive cells in various stages of KS. *A* and *B*, hematoxylin-eosin (HE) staining *(A)* and double immunohistochemical staining *(B)* of vascular endothelial cell growth factor receptor 3 (VEGFR-3) *(blue)* and latency-associated nuclear antigen (LANA) *(brown)* in serial sections of patch-stage KS. Original magnification, ×400. *C* and *D*, HE staining *(C)* and double immunohistochemical analysis *(D)* of VEGFR-3 *(blue)* and LANA *(red)* in serial sections of plaque-stage KS. Arrowheads indicate vascular endothelial cells. Original magnification, ×400. *E* and *F*, Double immunohistochemical analysis of VEGFR-3 *(blue)* and LANA *(red)* in nodular-stage KS. Original magnifications, ×100 *(E)* and ×400 *(F)*.

stage in KS lesions and that infection may induce an abnormal extension of endothelial cells and an enlargement of blood vessels, resulting in a relatively high number of KSHV copies.

DISCUSSION

In the present study, we evaluated numbers of viral copies and numbers of KSHV-infected cells in KSHV-associated diseases using real-time quantitative PCR and a computerized-image analytical method. The predicted number of KSHV copies was 3.2 viral copies/cell. The expression of ORF50 protein was rare or nonexistent in KS lesions, which suggests that latently infected cells were proliferating in KS lesions. In MCD samples, 25% of KSHV-infected cells expressed ORF50 protein, which implies that the lytic replication of KSHV was frequent in MCD lesions. To our knowledge, this is the first study describing both numbers of viral copies and numbers of virus-infected cells in pathologic samples from KSHV-associated disease lesions.

The combination of real-time PCR and computerized-image analysis allowed the prediction of numbers of viral copies per infected cell in each KSHV-associated disease. Predicted copy numbers per infected cell are listed in table 3. KS lesions might contain 0.27–5.89 viral copies/cell (average, 3.22 viral copies/cell) of KSHV. KSHV-associated solid lymphoma cells might contain >10 viral copies/cell. These numbers were close to the ones reported for KS cells (1 viral copy/cell) and PEL cells (50 viral copies/cell) [18, 19]. Because almost all KS cells express

LANA, a KS cell should have >1 copy of the virus. One molecule of LANA binds to 1 copy of the KSHV genome on chromosomes of host cells [34]. Immunohistochemical staining produces several dots of LANA in the nucleus of every KS cell [4, 6]. Thus, it is not surprising that a KS cell has several copies of KSHV. Like KS cells, PEL and KSHV-associated solid lymphoma cells exhibited several dots of LANA staining in their nucleus by immunohistochemical analysis, which suggests that PEL and KSHV-associated solid lymphoma cells also have several copies per cell. However, numbers of viral copies in PEL and KSHV-associated solid lymphoma cells were obviously higher than those in KS cells. One reason for that was that 3% of KSHV-associated solid lymphoma cells expressed ORF50 protein, which implies that a small population of lymphoma cells was in the lytic phase, whereas cells expressing ORF50 protein were very rare (<0.1%) in KS cells (table 3). These data suggest that there might be different systems involved in the maintenance or replication of viruses between KSHV-infected lymphoma cells and KS cells. KSHV-positive cells contained 3.38 viral copies/cell in MCD. This number seemed to be lower than what we expected, given that one-fourth of KSHV-infected cells expressed ORF50 protein. We could not determine numbers of viral copies in MCD, because numbers of viral copies might vary among cases, and we examined the virus titer in only one MCD sample. Further studies are definitely required to determine numbers of viral copies in MCD.

Our double immunohistochemical analysis revealed that flat endothelial cells of atypical vessels in early KS lesions expressed both LANA and VEGFR-3. It was difficult to distinguish KS cells from non-KS endothelial cells strictly in HE-stained sections of early KS lesions. VEGFR-3 is a useful marker for KS cells [33]. Our data suggest that a large proportion of extended endothelial cells in the patch stage of KS and KS spindle cells were already infected with KSHV. Because lytic protein expression was also rare during the patch stage, KSHV infected these cells latently. Thus, KSHV infection may be established in endothelial cells at a very early stage in KS lesions. We suggest that this is one of the reasons why numbers of KSHV copies in patch-stage lesions were similar to those in nodular-stage lesions of classic KS in real-time PCR results (figure 3).

Computerized-image analysis has been used by several groups to count cells in immunohistochemically stained sections [35–37]. Technically, our image analysis method was much easier than previously reported ones, in that (1) image files did not need to be captured at high magnification—relatively low magnifications (×40–×100, not ×400) are preferred; (2) splitting of images to red, green, and blue and counting of cells were done automatically; (3) tracing positive and negative cells could be easily visually confirmed; (4) it took only a few minutes to analyze an image; and (5) ImageJ is freeware. The unique features of the present study involve the combination of real-time PCR and computerized-image analysis. Real-time PCR is a powerful tool for measuring numbers of viral copies quickly and easily. However, every pathologic sample contains various numbers of normal cells, and it is impossible to extract DNA strictly from lesions in pathologic samples. Therefore, when DNA is extracted from pathologic samples that contain virus-infected cells, extracted DNA will contain not only DNA from virus-infected cells but also DNA from uninfected cells. Almost all studies that use real-time PCR encounter this limitation. Immunohistochemical analysis and in situ hybridization (ISH) are useful techniques that allow the localization of virus-infected cells. However, immunohistochemical analysis and ISH are not quantitative. Indeed, signal intensity does not correlate with copy number of the molecules or nucleotides, because signal intensity in immunohistochemical analysis and ISH differs among experiments and slides and depends on the conditions of staining or hybridization, such as incubation time, washing, temperature, fixation, and buffer. By combining real-time PCR and computerized-image analysis, the determination of relatively accurate virus numbers in infected cells becomes possible. Numbers of viral copies can be measured using real-time PCR, and numbers of virus-infected cells can be estimated with computerized-image analysis. Both results are required to assess numbers of viral copies in a virus-infected cell. In the present study, we analyzed 1 or a few pictures per slide using computerized-image analysis. Examination of a whole slide would be ideal; however, it is difficult to scan a whole slide using a high-resolution objective lens, but that may be available in the near future using, for example, a virtual slide system. In conclusion, the combination of real-time PCR and computerized-image analysis provides a useful tool for the prediction of numbers of viral copies in virus-associated diseases and of numbers of copies of certain molecules in a cell.

References

1. Moore PS, Chang Y. Kaposi's sarcoma-associated herpesvirus. In: Knipe DM, Howley PM, eds. Fields virology. Vol 2, 4th ed. Philadelphia: Lippincott, Williams & Wilkins, **2001**:2803–33.
2. Moore PS, Chang Y. Detection of herpesvirus-like DNA sequences in Kaposi's sarcoma in patients with and without HIV infection. N Engl J Med **1995**; 332:1181–5.
3. Dupin N, Grandadam M, Calvez V, et al. Herpesvirus-like DNA sequences in patients with Mediterranean Kaposi's sarcoma. Lancet **1995**; 345:761–2.
4. Katano H, Sato Y, Kurata T, Mori S, Sata T. High expression of HHV-8-encoded ORF73 protein in spindle-shaped cells of Kaposi's sarcoma. Am J Pathol **1999**; 155:47–52.
5. Dupin N, Fisher C, Kellam P, et al. Distribution of human herpesvirus-8 latently infected cells in Kaposi's sarcoma, multicentric Castleman's disease, and primary effusion lymphoma. Proc Natl Acad Sci USA **1999**; 96:4546–51.
6. Parravicini C, Chandran B, Corbellino M, et al. Differential viral protein expression in Kaposi's sarcoma-associated herpesvirus-infected diseases: Kaposi's sarcoma, primary effusion lymphoma, and multicentric Castleman's disease. Am J Pathol **2000**; 156:743–9.
7. Nador RG, Cesarman E, Chadburn A, et al. Primary effusion lym-

phoma: a distinct clinicopathologic entity associated with the Kaposi's sarcoma-associated herpes virus. Blood **1996**; 88:645–56.
8. Katano H, Suda T, Morishita Y, et al. Human herpesvirus 8-associated solid lymphomas that occur in AIDS patients take anaplastic large cell morphology. Mod Pathol **2000**; 13:77–85.
9. Chadburn A, Hyjek E, Mathew S, Cesarman E, Said J, Knowles DM. KSHV-positive solid lymphomas represent an extra-cavitary variant of primary effusion lymphoma. Am J Surg Pathol **2004**; 28:1401–16.
10. Soulier J, Grollet L, Oksenhendler E, et al. Kaposi's sarcoma-associated herpesvirus-like DNA sequences in multicentric Castleman's disease. Blood **1995**; 86:1276–80.
11. Suda T, Katano H, Delsol G, et al. HHV-8 infection status of AIDS-unrelated and AIDS-associated multicentric Castleman's disease. Pathol Int **2001**; 51:671–9.
12. Sun R, Lin SF, Staskus K, et al. Kinetics of Kaposi's sarcoma-associated herpesvirus gene expression. J Virol **1999**; 73:2232–42.
13. Rivas C, Thlick AE, Parravicini C, Moore PS, Chang Y. Kaposi's sarcoma-associated herpesvirus LANA2 is a B-cell-specific latent viral protein that inhibits p53. J Virol **2001**; 75:429–38.
14. Rainbow L, Platt GM, Simpson GR, et al. The 222- to 234-kilodalton latent nuclear protein (LNA) of Kaposi's sarcoma-associated herpesvirus (human herpesvirus 8) is encoded by orf73 and is a component of the latency-associated nuclear antigen. J Virol **1997**; 71:5915–21.
15. Lukac DM, Kirshner JR, Ganem D. Transcriptional activation by the product of open reading frame 50 of Kaposi's sarcoma-associated herpesvirus is required for lytic viral reactivation in B cells. J Virol **1999**; 73: 9348–61.
16. Zhu FX, Cusano T, Yuan Y. Identification of the immediate-early transcripts of Kaposi's sarcoma-associated herpesvirus. J Virol **1999**; 73: 5556–67.
17. Katano H, Sato Y, Kurata T, Mori S, Sata T. Expression and localization of human herpesvirus 8-encoded proteins in primary effusion lymphoma, Kaposi's sarcoma, and multicentric Castleman's disease. Virology **2000**; 269:335–44.
18. Cesarman E, Chang Y, Moore PS, Said JW, Knowles DM. Kaposi's sarcoma-associated herpesvirus-like DNA sequences in AIDS-related body-cavity-based lymphomas. N Engl J Med **1995**; 332:1186–91.
19. Lallemand F, Desire N, Rozenbaum W, Nicolas JC, Marechal V. Quantitative analysis of human herpesvirus 8 viral load using a real-time PCR assay. J Clin Microbiol **2000**; 38:1404–8.
20. White IE, Campbell TB. Quantitation of cell-free and cell-associated Kaposi's sarcoma-associated herpesvirus DNA by real-time PCR. J Clin Microbiol **2000**; 38:1992–5.
21. Campbell TB, Borok M, Gwanzura L, et al. Relationship of human herpesvirus 8 peripheral blood virus load and Kaposi's sarcoma clinical stage. AIDS **2000**; 14:2109–16.
22. Tedeschi R, Enbom M, Bidoli E, Linde A, De Paoli P, Dillner J. Viral load of human herpesvirus 8 in peripheral blood of human immunodeficiency virus-infected patients with Kaposi's sarcoma. J Clin Microbiol **2001**; 39:4269–73.
23. Quinlivan EB, Zhang C, Stewart PW, Komoltri C, Davis MG, Wehbie RS. Elevated virus loads of Kaposi's sarcoma–associated human herpesvirus 8 predict Kaposi's sarcoma disease progression, but elevated levels of human immunodeficiency virus type 1 do not. J Infect Dis **2002**; 185:1736–44.
24. Boivin G, Cote S, Cloutier N, Abed Y, Maguigad M, Routy JP. Quantification of human herpesvirus 8 by real-time PCR in blood fractions of AIDS patients with Kaposi's sarcoma and multicentric Castleman's disease. J Med Virol **2002**; 68:399–403.
25. Engels EA, Biggar RJ, Marshall VA, et al. Detection and quantification of Kaposi's sarcoma-associated herpesvirus to predict AIDS-associated Kaposi's sarcoma. AIDS **2003**; 17:1847–51.
26. Song J, Yoshida A, Yamamoto Y, et al. Viral load of human herpesvirus 8 (HHV-8) in the circulatory blood cells correlates with clinical progression in a patient with HHV-8-associated solid lymphoma with AIDS-associated Kaposi's sarcoma. Leuk Lymphoma **2004**; 45:2343–7.
27. Renne R, Zhong W, Herndier B, et al. Lytic growth of Kaposi's sarcoma-associated herpesvirus (human herpesvirus 8) in culture. Nat Med **1996**; 2:342–6.
28. Katano H, Hoshino Y, Morishita Y, et al. Establishing and characterizing a CD30-positive cell line harboring HHV-8 from a primary effusion lymphoma. J Med Virol **1999**; 58:394–401.
29. Chang Y, Cesarman E, Pessin MS, et al. Identification of herpesvirus-like DNA sequences in AIDS-associated Kaposi's sarcoma. Science **1994**; 266:1865–9.
30. Katano H, Sato Y, Itoh H, Sata T. Expression of human herpesvirus 8 (HHV-8)-encoded immediate early protein, open reading frame 50, in HHV-8-associated diseases. J Hum Virol **2001**; 4:96–102.
31. Hong YK, Foreman K, Shin JW, et al. Lymphatic reprogramming of blood vascular endothelium by Kaposi sarcoma-associated herpesvirus. Nat Genet **2004**; 36:683–5.
32. Wang HW, Trotter MW, Lagos D, et al. Kaposi sarcoma herpesvirus-induced cellular reprogramming contributes to the lymphatic endothelial gene expression in Kaposi sarcoma. Nat Genet **2004**; 36:687–93.
33. Weninger W, Partanen TA, Breiteneder-Geleff S, et al. Expression of vascular endothelial growth factor receptor-3 and podoplanin suggests a lymphatic endothelial cell origin of Kaposi's sarcoma tumor cells. Lab Invest **1999**; 79:243–51.
34. Ballestas ME, Chatis PA, Kaye KM. Efficient persistence of extrachromosomal KSHV DNA mediated by latency-associated nuclear antigen. Science **1999**; 284:641–4.
35. Chantrain CF, DeClerck YA, Groshen S, McNamara G. Computerized quantification of tissue vascularization using high-resolution slide scanning of whole tumor sections. J Histochem Cytochem **2003**; 51:151–8.
36. Johansson AC, Visse E, Widegren B, Sjogren HO, Siesjo P. Computerized image analysis as a tool to quantify infiltrating leukocytes: a comparison between high- and low-magnification images. J Histochem Cytochem **2001**; 49:1073–79.
37. Lehr HA, Mankoff DA, Corwin D, Santeusanio G, Gown AM. Application of photoshop-based image analysis to quantification of hormone receptor expression in breast cancer. J Histochem Cytochem **1997**; 45: 1559–65.

研究成果の刊行に関する一覧表

1．書籍

該当なし

2．雑誌

発表者氏名	論文タイトル名	発表誌名	巻号	ページ	出版年
Yamada, T., Watanabe, N., Nakamura, T and Iwamoto, A.	Antibody-dependent cellular cytotoxicity via a humoral immune epitope of Nef protein expressed on the cell surface.	J. Immunology.	172	2401-6	2004
Furutsuki T, Hosoya N, Kawana-Tachikawa A, Tomizawa M, Odawara T, Goto M, Kitamura Y, Nakamura T, Kelleher AD, Cooper DA, Iwamoto A.	Frequent transmission of cytotoxic-T-lymphocyte escape mutants of human immunodeficiency virus type 1 in the highly HLA-A24-positive Japanese population.	J Virol	78	8437-45	2004
D Zhu, H Taguchi-Nakamura, M Goto, T Odawara, T Nakamura, H Yamada, H Kotaki, W Sugiura, A Iwamoto & Y Kitamura	Influence of single-nucleotide polymorphisms in the multidrug resistance-1 gene on the cellular export of nelfinavir and its clinical implication for highly active antiretroviral therapy.	Antiviral Therapy	9	905-11	2004
Tomonari A, Takahashi S, Shimohakamada Y, Ooi J, Takasugi K, Ohno N, Konuma T, Uchimaru K, Tojo A, Odawara T, Nakamura T, Iwamoto A, Asano S.	Unrelated cord blood transplantation for a human immunodeficiency virus-1-seropositive patient with acute lymphoblastic leukemia.	Bone Marrow Transplant	36	261-262	2005
T. Maeda, T. Fujii, T. Matsumura, T. Endo, T. Odawara, D. Itoh, Y Inoue, T. Okubo, A. Iwamoto, T. Nakamura.	AIDS-related cerebral toxoplasmosis with hypertense foci on T1-weighted MR images: A case report.	J. Infect.	in press		

Antibody-Dependent Cellular Cytotoxicity via Humoral Immune Epitope of Nef Protein Expressed on Cell Surface[1]

Takeshi Yamada,[2]* Nobukazu Watanabe,† Tetsuya Nakamura,‡ and Aikichi Iwamoto[3]*‡

Antibodies against various proteins of HIV type 1 (HIV-1) can be detected in HIV-1-infected individuals. We previously reported that the level of Ab response against one Nef epitope is correlated with HIV-1 disease progression. To elucidate the mechanism for this correlation, we examined Ab-dependent cellular cytotoxicity (ADCC) against target cells expressing Nef. We observed efficient cytotoxicity against Nef-expressing target cells in the presence of patient plasma and PBMCs. This ADCC activity was correlated with the dilution of plasma from HIV-1-infected patients. Addition of a specific synthetic peptide (peptide 31: FLKEKGGLE) corresponding to the Nef epitope reduced cell lysis to ~50%. These results suggest that PBMCs of HIV-1-infected patients may exert ADCC via anti-Nef Abs in the patients' own plasma and serve as a mechanism used by the immune system to regulate HIV-1 replication. ***The Journal of Immunology,*** **2004, 172: 2401–2406.**

Highly active antiretroviral therapy dramatically suppresses HIV-1 replication and has thereby contributed to decrease the incidence of AIDS-related opportunistic infections and subsequent mortality (1, 2). However, elimination of HIV-1 from infected individuals has not yet been achieved by highly active antiretroviral therapy alone (3–5). Therefore, the development of different therapeutic approaches is mandatory.

Ab-dependent cellular cytotoxicity (ADCC)[4] as well as CTL play an important role in protective immunity against viral infections (6, 7). ADCC can inhibit viral replication and cell-to-cell infection by killing HIV-1-infected cells before maturation of virus particles (8, 9). Therefore, ADCC activity could benefit the prevention of disease progression. In early studies, Rook et al. (10) and Ljunggren et al. (11) demonstrated that sera from HIV-1-infected individuals were able to mediate ADCC against HIV-1-infected T cells, and there was a positive correlation between ADCC activity and disease progression. When HIV-1-infected cells produce virus particles, viral envelope glycoproteins are abundantly exposed to the cell surface through the plasma membrane. In fact, ADCC via Abs against gp120 or gp41, HIV-1 envelope protein, has been well documented (12–20). It has been described that gp120 or gp120/41-specific ADCC correlates with rate of disease progression (19, 21). But, in contrast, ADCC via envelope proteins could potentially kill the uninfected $CD4^+$ T cells with free viral envelopes on their surface, and therefore ADCC could contribute to depletion of $CD4^+$ T cells and AIDS pathogenesis (22, 23). In addition, gp120 is prone to high frequency of mutations; thereby, viral escape mutants may evolve easily (24–26). In view of these disadvantages, envelope proteins appear to be unsuitable as targets for ADCC against the progression of disease in HIV-1-infected patients. Conserved proteins may be better targets if one considers ADCC as a durable therapeutic weapon against HIV-1. With regard to this, Gag and Pol are very conserved proteins, and if their epitopes were expressed on the cell surface, these proteins could be good candidates for specific ADCC. Rook et al. (10) described that Ab reactivity with the p24 (Gag) protein of patient's serum correlates inversely with disease progression. It has been reported that Gag proteins are expressed on the cell surface (27, 28); nevertheless, the inductions of ADCC via Gag have never been succeeded (29). And, furthermore, there has been no evidence that Pol proteins are expressed on the HIV-1-infected cells; therefore, Pol Ags could not be exposed to the extracellular enviroment as ADCC target. Thus, the contribution of other HIV-1 proteins except envelope proteins to ADCC has remained unclear.

Nef protein is an HIV-1 accessory protein with important roles for pathogenesis of HIV-1 infection (30–35). Nef protein is partially expressed on the surface of HIV-1-infected cells (36–38). We previously reported that highly conserved amino acid residues (FLKEKGGLE) are expressed on the surface of HIV-1-infected cells. The peptide residues served as an epitope for Ab response, and the plasma level of the Abs against the epitope was correlated with HIV-1 disease progression (39, 40). To elucidate the mechanism of this correlation, we studied ADCC activities using patients' peripheral mononuclear cells (PBMCs) and a patient's plasma, which contained high amount of anti-Nef Abs. We also analyzed characteristics of patients' NK cells that should be the key player in ADCC against virus-induced target cells.

Materials and Methods

Cells

Five HIV-1-infected subjects whose PBMCs were used as effector cells for the ADCC assay are listed in Table I. PBMCs were freshly isolated by centrifuging heparinized blood over Ficoll-Hypaque (Meneki-seibutsuken, Gunma, Japan). PBMCs were counted and adjusted to the concentration of 2×10^6 cells/ml in RPMI 1640 medium supplemented with 10% heat-inactivated FCS (RPMI 10). A portion of the cells was used for phenotypic analysis using flow cytometry. For the flow cytometric analysis of NK

*Division of Infectious Diseases, Advanced Clinical Research Center, †Division of Cell Processing, and ‡Department of Infectious Disease and Applied Immunology, Institute of Medical Science, University of Tokyo, Minato-ku, Tokyo, Japan

Received for publication June 23, 2003. Accepted for publication December 1, 2003.

The costs of publication of this article were defrayed in part by the payment of page charges. This article must therefore be hereby marked *advertisement* in accordance with 18 U.S.C. Section 1734 solely to indicate this fact.

[1] This work was supported in part by grants from the Ministry of Health and Welfare of Japan and the Health Sciences Foundation.

[2] Current address: Department of Microbiology, Graduate School of Medicine, University of Tokyo, 7-3-1 Hongo, Bunkyo-ku, Tokyo 113-0033, Japan.

[3] Address correspondence and reprint requests to Dr. Aikichi Iwamoto, Division of Infectious Diseases, Advanced Clinical Research Center, Institute of Medical Science, University of Tokyo, 4-6-1 Shirokanedai, Minato-ku, Tokyo 108-8639, Japan. E-mail address: aikichi@ims.u-tokyo.ac.jp

[4] Abbreviations used in this paper: ADCC, Ab-dependent cellular cytotoxicity; LTNP, long-term nonprogressor.

0022-1767/04/$02.00

Table I. *Patient profiles*

Patient	Age	Sex	$CD4^+$ Count (cells/μl)	$CD8^+$ Count (cells/μl)	NK Cell Count (cells/μl)	% NK Cell in FBMC	HIV RNA (copies/ml)[a]	Antiretroviral Drugs[b]
P1	37	M	754	996	155	8.0	<400	d4T + 3TC + NFV
P2	32	M	63	214	20	3.7	770	d4T + 3TC + NFV
P3	45	M	204	620	220	12.6	<400	AZT + ddC + IDV
P4	37	M	638	1034	102	5.7	<400	d4T + 3TC + NFV
P5	35	M	372	877	73	5.0	2200	AZT + ddC + IDV

[a] Amplicor HIV monitor test (Roche Diagnostics Systems, Somerville, NJ).
[b] AZT, zidovudine; d4T, stavudine; 3TC, lamivudine; ddC, zalcitabine; NFV, nelfinavir; IDV, indinavir.

cells, PBMC samples from another 40 HIV-1-positive subjects and 16 uninfected donors were included in this study.

For the ADCC assay, we used CEM-NK^R cells that were obtained through the AIDS Research and Reference Reagent Program, Division of AIDS, National Institute of Allergy and Infectious Diseases, National Institutes of Health from J. Corbeil (41). Nef proteins were expressed in these cells by using a recombinant Sendai virus system, which has been shown to express large amounts of heterologous recombinant proteins in 24 h after infection in suspension cells (42). CEM-NK^R cells were infected with SeV-Nef to express HIV-1 (NL43 strain) Nef proteins or wild SeV at a multiplicity of infection of 10 for 1 h at 37°C, as previously described (43), and cultured for 24 h in RPMI 10. These cells were designated CEM-NK^R-Nef or CEM-NK^R-mock cells, respectively.

Subjects and reagents

For ADCC assay, we used the plasmas from long-term nonprogressor 2, 5, and 6 (LTNP 2, 5, and 6), whose characterization was published previously (39). $Na_2[^{51}Cr]O_4$ was obtained from NEN Life Science Products (Boston, MA). mAbs N901 (NKH-1) (anti-CD56; FITC conjugated) and 3G8 (anti-CD16; PE) were obtained from Coulter (Miami, FL). mAbs SJ25C1 (anti-CD19; PerCP) and SK7 (anti-CD3; allophycocyanin) were obtained from BD Immunocytometry Systems (San Jose, CA). mAb δG9 (anti-perforin) was a generous gift of E. Podack (University of Miami, Miami, FL). δG9 was conjugated with FITC in our laboratory. Nine-mer peptide 31 (=FLKEKGGLE) and control peptide (=GGGGGGGGG) were synthesized using a Multipin peptide synthesis kit (Chiron Mitotopes, Clayton, Victoria, Australia). The yields were analyzed by gas-liquid chromatography to confirm the correct synthesis.

Immunofluorescent staining

For analysis of Sendai virus-infected CEM-NK^R cells, cells (10^5) were centrifuged over silan-coating glass coverslips (DAKO, Carpenteria, CA), fixed with 2% paraformaldehyde in PBS for 5 min, blocked with BlockAce (Snow-Brand, Tokyo, Japan) for 30 min, and incubated for 1 h with plasma of LTNP 5 1/2.5 diluted in PBS. Then cells were incubated for 30 min with FITC-conjugated goat anti-human Igs (IgG, IgA, and IgM) $F(ab')_2$ (BioSource International, Camarillo, CA) after wash with PBS, and were mounted in 85% glycerol, 10 mM of Tris-HCl (pH 8), and 5% *n*-propylgallate. These stained cells were inspected with a confocal microscope (MRC 1024; Bio-Rad, Hercules, CA).

ADCC assays

ADCC assays were performed in 200 μl, total volume. Patient plasma used in the ADCC assay was incubated for 30 min at 56°C to inactivate the complement system. Plasmas from randomly selected healthy donors were used as control. A total of 1×10^6 target cells was labeled by incubation with medium containing $Na_2[^{51}Cr]O_4$ (0.5 mCi/ml) at 37°C for 1 h. Cells were washed three times with plain RPMI 1640 medium and resuspended in RPMI 10 at 2×10^5 cells/ml. A total of 50 μl of resuspended cells was added to each well of a 96-well microtiter plate (U bottom). Then, 50 μl of heat-inactivated healthy or patient's plasma diluted to 1/2.5 (thus, final concentration equals to 10^{-1} of original in 200 μl, total volume) in RPMI 10 was added to the plate before incubating for 30 min at 37°C. For the dilution assay of plasma, final concentration of plasma was adjusted to 10^{-1}, 10^{-2}, 10^{-3}, and 10^{-4} of original with RPMI 10, respectively. After incubation, either 100 μl of patients' PBMCs (2×10^6 cells/ml) (for sample count), 100 μl of RPMI 10 containing 2% Triton solution (for maximum count), or 100 μl of RPMI 10 (for spontaneous release count) was added to each well. The mixtures of reaction were incubated at 37°C in a humidified 5% CO_2 atmosphere for 4 h as in previous reports (8, 41). A total of 100 μl of supernatant was collected from each well, and γ emission was counted using a gamma counter. The percentage of dead cells was calculated using the following formula: cell death (%) = 100 × (sample count − spontaneous release)/(maximum count − spontaneous release).

Blocking of ADCC by peptide 31

After diluted plasma was added with 0, 10, or 100 μg/ml peptide 31 (=FLKEKGGLE) or 100 μg/ml of control peptide (=GGGGGGGGG), 50 μl of the solution was added to resuspended target cells. ADCC assay was performed as above.

Flow cytometric analysis

For analysis of NK cell subsets, we used the following Ab combinations: 1) FITC-conjugated anti-CD56, PE anti-CD16, PerCP anti-CD19, allophycocyanin anti-CD3; 2) FITC anti-perforin, PE anti-CD56, PE anti-CD16, PerCP anti-CD19, allophycocyanin anti-CD3. For phenotypic analysis of NK cells, PBMCs were suspended in 50 μl of culture medium, and stained with Ab combination 1, for 20 min on ice. After incubation, cells were washed twice with cold PBS. Cells were resuspended in 200 μl of PBS containing 0.5% formaldehyde. For intracellular staining of perforin, cells were stained with Ab combination 2 (without anti-perforin Ab) for 20 min. After incubation, cells were washed twice with cold PBS, and resuspended in 100 μl of PBS. After addition of 100 μl of 4% formaldehyde and incubation for 20 min at room temperature, cells were pelleted and supernatants were removed. Cells were washed once with PBS/0.5% BSA/1 mM of sodium azide (PBS/BSA/azide buffer), and resuspended in 150 μl of permeabilization buffer (PBS/BSA/azide buffer containing 0.5% saponin). After pipetting gently to mix and incubating for 10 min at room temperature, cells were pelleted and supernatant was removed. A total of 25 μl of permeabilization buffer containing the appropriate amount of Abs against intracellular perforin was added to the cell pellets and incubated at room temperature for 30 min in the dark. Cells were washed once with 0.5 ml of permeabilization buffer and once with 1 ml of PBS/BSA/azide buffer. Finally, cells were suspended in 200 μl of PBS/BSA/azide buffer. All samples were kept at 4°C and protected from light until analysis on the flow cytometer.

Six-parameter flow cytometric analysis was done on a FACSCalibur flow cytometer (BD Immunocytometry Systems) using CellQuest software (BD Immunocytometry Systems) with FITC, PE, PerCP, and allophycocyanin as the four fluorescent parameters. FlowJow software (Tree Star, San Carlos, CA) was used to make configurations. Light scatter gates were designed to include only lymphocytes, and up to 100,000 events in this gate were collected. The absolute lymphocyte count was determined from the complete blood count. The number of NK cells per microliter of whole blood was calculated by multiplying the fraction of lymphocytes that were $CD16^+$ or $CD56^+$ by the absolute lymphocyte per microliter of blood. For analysis and display of statistical comparisons, we used JMP software for the Apple Macintosh (SAS Institute, Cary, NC). Comparisons of distributions were performed by the nonparametric two-sample Wilcoxon rank test.

Results

Nef protein expression on the cell surface infected with SeV-Nef

LTNP 5 in the previous study had a high titer of the Abs against peptide 31 (39). When CEM-NK^R-Nef cells fixed with paraformaldehyde were stained with diluted plasma from healthy donor or LTNP 5, and FITC-conjugated anti-human Ig secondary Abs, positive fluorescent signals were given on the surface of CEM-NK^R-Nef cells by plasma from LTNP 5, but not from a healthy donor

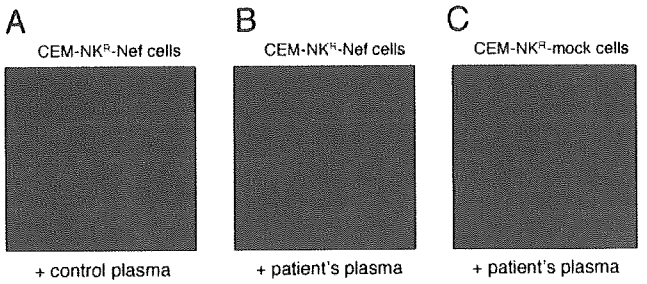

FIGURE 1. Immunological staining of CEM-NK^R cells infected with SeV-Nef (CEM-NK^R-Nef cells). Cells were stained with 1/2.5 diluted plasma and FITC-conjugated anti-human Ig secondary Abs. The stained cells were observed by confocal microscopy. *A*, CEM-NK^R-Nef cells stained with plasma of a healthy donor. *B*, CEM-NK^R-Nef cells stained with plasma from LTNP 5. *C*, CEM-NK^R-mock cells stained with plasma from LTNP 5.

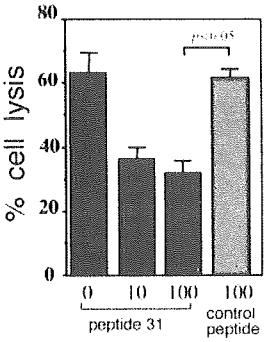

FIGURE 3. Inhibition of ADCC by peptide 31. Percentage of cell lysis by PBMCs of P3 was examined by ADCC assay in the presence of peptide 31 (■) or control peptide (hatched column) at an E:T ratio of 20:1. Data are shown as the mean of triplicate determinations (bars represent SDs). There is a significant difference between peptide 31 and control peptide at the concentration of 100 μg/ml (Student's t test, $p < 0.05$).

(Fig. 1, *A* and *B*). Plasma from LTNP 5 did not recognize proteins on the cell surface of CEM-NK^R-mock cell (Fig. 1*C*).

ADCC assay

An ADCC assay was conducted using plasma from LTNPs (LTNP 2, 5, and 6) (39) and PBMCs of either a healthy volunteer or from a patient 1–5 whose profiles are provided in Table I. As shown in Fig. 2*A*, CEM-NK^R-Nef incubated with plasma of LTNP 5 (final concentration, 10^{-1} of original) was efficiently lysed with PBMCs of a healthy volunteer at an E:T ratio of 20:1 (mean percentage of cell lysis, 58%) and 50:1 (66%). When the E:T ratio was lowered to 5:1, percentage of cell lysis decreased to 30% (Fig. 2*A*). The plasmas from LTNP 2, 5, and 6 (final concentration, 10^{-1} of original) induced ADCC activity via Nef, and the plasma of LTNP 6 indicated lower activity compared with that of LTNP 2 or LTNP 5 (Fig. 2*B*). Cytotoxic activity against CEM-NK^R-Nef was observed when PBMCs of five HIV-1-infected patients (p1–5) were used as effector cells at an E:T ratio of 20:1 (Fig. 2*C*). This cytotoxicity was specific to plasma of HIV-1-infected patients, because cell lysis was less than 10% when plasma from a healthy donor was used instead of patient plasma (Fig. 2*C*). In addition, the observation that dilution of patient plasma reduced the percentage of CEM-NK^R-Nef cell lysis (Fig. 2*D*) also suggested that lysis was mediated by the Ab in the plasma. To examine whether the cell lysis is specific to Nef, we added synthetic peptide 31 to the mixture of ^{51}Cr-labeled CEM-NK^R-Nef, PBMCs of patient 3, and LTNP 5 plasma at an E:T ratio of 20:1. Addition of 10 or 100 μg/ml peptide 31 decreased the percentage of cell lysis by 42 or 48% when compared with cell lysis without peptide 31, respectively, whereas addition of 100 μg/ml of control peptide did not show any effect on cytotoxicity (Fig. 3).

NK cells of HIV-1-infected patients

We analyzed NK cells in the peripheral blood using flow cytometry. NK cells were defined as CD3$^-$, CD19$^-$, CD16$^+$, or CD56$^+$ lymphocyte (44). PBMCs from 41 HIV-1-infected patients and 16 healthy donors were examined. There was a significant difference between HIV-1-infected patients and normal controls in total counts of NK cells (mean ± SD = 131 ± 85 and 198 ± 87 cells/μl, respectively, $p = 0.014$) (Fig. 4*A*). When HIV-1-infected individuals were divided into two groups by CD4$^+$ T cell counts (CD4 ≥ 200 or CD4 < 200 cells/μl), there was no significant difference between these two groups in absolute counts of NK cells (CD4 ≥ 200 and CD4 < 200 cells/μl; mean ± SD = 125 ± 94 and 142 ± 82 cells/μl, respectively, $p = 0.643$). For the functional analysis of NK cells, we next examined the expression of intracellular perforin in NK cells of HIV-1-infected patients. As shown in Fig. 4*B*, there was no significant difference between HIV-1-infected patients and healthy controls in frequency of perforin high-positive cell (%) of total NK cells (CD4 ≥ 200, CD4 < 200 cells/μl, and healthy controls; mean ± SD = 83 ± 12, 90 ± 6, and

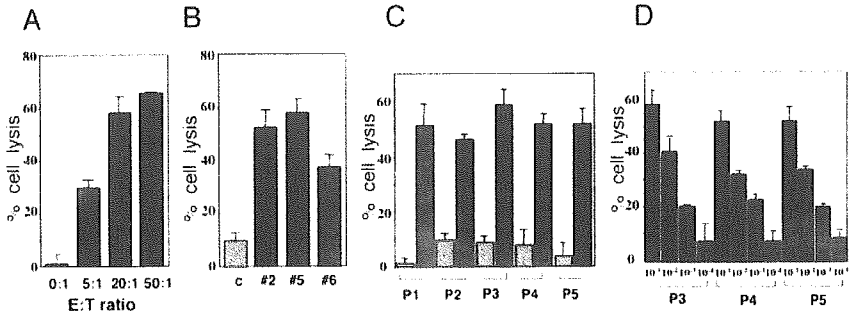

FIGURE 2. ADCC assay using diluted plasma, PBMCs, and radiorabeled CEM-NK^R-Nef. The values are given as percentage of specific cell lysis = 100 × (sample count − spontaneous release)/(maximum count − spontaneous release). *A*, Various E:T ratio with healthy donor PBMCs in the presence of plasma from LTNP 5. *B*, Plasma from a healthy donor (hatched column) or LTNPs (LTNP 2, 5, and 6) (■) at an E:T ratio of 20:1 with healthy donor PBMCs. *C*, PBMCs from five patients (P1-P5, Table I) at an E:T ratio of 20:1 in the presence of either plasma from a healthy donor (hatched column) or LTNP 5 (■) in *C*. *D*, Plasma Ab titration. Percentage of cell lysis by PBMCs from patient P3, P4, or P5 was examined with serially diluted plasma from LTNP 5 at an E:T ratio of 20:1. The values along the x-axis represent final concentration, 10^{-1}~10^{-4} of original plasma. Data are shown as the mean of triplicate determinations (bars represent SDs).

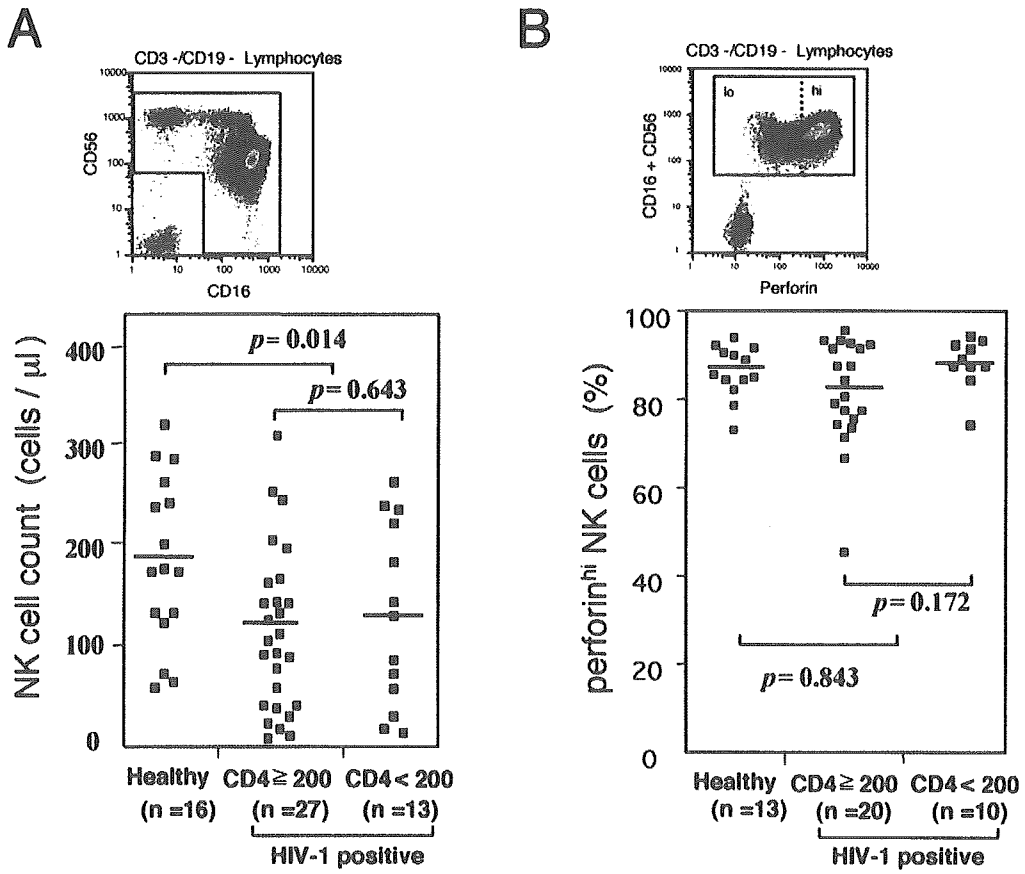

FIGURE 4. Flow cytometric analysis of NK cells. NK cells were defined by $CD3^-$, $CD19^-$, $CD16^+$, or $CD56^+$ expression. *Upper panels*, Show flow cytometry profiles gated on $CD3^-$ and $CD19^-$ lymphocytes. NK cells were gated by red filled line. *A*, *Lower panel*, Comparison of NK cell counts was conducted between 16 healthy donors and 40 HIV-1-positive individuals. *B*, *Upper panel*, NK cells are distingushed between perforin high/positive (hi) and low (lo) populations by red dotted line. *Lower panel*, Frequency of perforin high-positive cells (%) of total NK cells for each donor was calculated. Comparison was conducted between 13 healthy donors and 30 HIV-1-positive individuals. Median values are shown as bars.

88 ± 6%, respectively), suggesting that NK cells in HIV-1-infected patients were as functionally active as those in non-HIV-1-infected individuals.

Discussion

In a previous report, we showed that the progression of disease in HIV-1-infected patients was correlated with Ab titers against peptide 31 (39). In an effort to elucidate the mechanism for this correlation, we studied the role of ADCC against peptide 31 in this study. The interaction between plasma Abs of LTNP 5 and Nef proteins was specific (Fig. 1). We showed that PBMCs from HIV-1-infected donors as well as healthy donors could exert specific ADCC against the cells expressing Nef protein ($CEM\text{-}NK^R$-Nef cells) with patient's plasma even in the face of less than normal NK cell count (Table 1; Fig. 2, *A*, *B*, and *C*). Thus, the ADCC activity may contribute to the elimination of HIV-1-infected cells in vivo. Because ADCC activity is dependent on the titer of plasma Ab (Fig. 2*D*), the lower activity of LTNP 6 (Fig. 2*B*) could be attributed to the lower titer of Ab against Nef epitope compared with LTNP 2 or 5, based on our previous data (39). The ADCC activity was inhibited up to ~50% by peptide 31 compared with control peptide (Fig. 3), suggesting that specific Abs against peptide 31 may contribute substantially to eliminate the HIV-1-infected cells. However, other Nef-derived peptides may also contribute to the residual 50% activity as epitopes we have not yet isolated. It was previously shown that selective down-regulation of MHC class I molecules protects HIV-1-infected cells from CTL and NK cells (45–49). In contrast, ADCC via Abs against the conserved cell surface HIV-1 epitopes such as peptide 31 may be an alternative armor against HIV-1 infection.

Although percentages of NK cells varied in the five patients examined (3.7~12.6%) (Table I), they showed almost the same levels of ADCC activity (Fig. 2*C*). This result may be due to the high E:T ratio that we used in the cytotoxicity assay (Fig. 2*A*); however, it is possible that ADCC activity may be retained until late in the clinical stage, as previously reported (50, 51). Flow cytometric analysis revealed a reduction of total NK cell counts in HIV-1-infected individuals, similar to the previous reports (52, 53) (Fig. 4*A*). There was no significant difference between the two groups of HIV-1-positive patients (CD4 ≥ 200 cells/μl and CD4 < 200 cells/μl); therefore, NK cells appear to be retained even late in the disease progression. With regard to Nef epitope expressing on the cell surface, we previously documented that HIV-1-infected cells were lysed by the combination of rabbit polyclonal Abs against peptide 31 and rabbit complements (39). Thus, we speculate that the level of Nef expression could be sufficient for the induction of ADCC via Nef epitope on the cell surface. However, it could be too difficult to estimate ADCC via Nef epitope with HIV-1-infected cells and patient's plasma because of the existence of abundant anti-envelope Abs as well as anti-Nef Abs in the plasma from HIV-1-infected patient.

We and others showed that HIV-1-specific CD8 T cells contain less perforin (54–56). NK cells may function as better effector cells in the HIV-1-infected individuals. Although the number of

NK cells was lower in HIV-1-infected patients than healthy controls, NK cells retained the high expression of perforin until late in the clinical course (Fig. 4*B*). Rukavina et al. (57) demonstrated that perforin expression significantly correlates with NK cytotoxicity against K562 cells. The fact that LTNPs had higher anti-peptide 31 Abs than progressors may indicate that ADCC against conserved cell surface HIV-1 epitopes such as peptide 31 may have favorable influence on the clinical course. Finally, therapeutic intervention that contributes to raise specific Ab levels against the conserved cell surface HIV-1 epitopes may prove to have a clinical benefit.

Acknowledgments

We thank Mieko Goto, Ai Kawana-Tachikawa, Mariko Tomizawa, and Naotoshi Kaji for their excellent technical assistance, and David Chao and Shinichiro Fuse for their kind reading of the manuscript.

References

1. Autran, B., G. Carcelain, T. S. Li, C. Blanc, D. Mathez, R. Tubiana, C. Katlama, P. Debre, and J. Leibowitch. 1997. Positive effects of combined antiretroviral therapy on $CD4^+$ T cell homeostasis and function in advanced HIV disease. *Science 277:112.*
2. Palella, F. J., Jr., K. M. Delaney, A. C. Moorman, M. O. Loveless, J. Fuhrer, G. A. Satten, D. J. Aschman, and S. D. Holmberg. 1998. Declining morbidity and mortality among patients with advanced human immunodeficiency virus infection: HIV Outpatient Study Investigators. *N. Engl. J. Med. 338:853.*
3. Chun, T. W., L. Stuyver, S. B. Mizell, L. A. Ehler, J. A. Mican, M. Baseler, A. L. Lloyd, M. A. Nowak, and A. S. Fauci. 1997. Presence of an inducible HIV-1 latent reservoir during highly active antiretroviral therapy. *Proc. Natl. Acad. Sci. USA 94:13193.*
4. Finzi, D., M. Hermankova, T. Pierson, L. M. Carruth, C. Buck, R. E. Chaisson, T. C. Quinn, K. Chadwick, J. Margolick, R. Brookmeyer, et al. 1997. Identification of a reservoir for HIV-1 in patients on highly active antiretroviral therapy. *Science 278:1295.*
5. Wong, J. K., M. Hezareh, H. F. Gunthard, D. V. Havlir, C. C. Ignacio, C. A. Spina, and D. D. Richman. 1997. Recovery of replication-competent HIV despite prolonged suppression of plasma viremia. *Science 278:1291.*
6. De Noronha, F., R. Baggs, W. Schafer, and D. Bolognesi. 1977. Prevention of oncornavirus-induced sarcomas in cats by treatment with antiviral antibodies. *Nature 267:54.*
7. Shore, S. L., T. L. Cromeans, and T. J. Romano. 1976. Immune destruction of virus-infected cells early in the infectious cycle. *Nature 262:695.*
8. Hildreth, J. E., R. Hampton, and N. A. Halsey. 1999. Antibody-dependent cell-mediated cytotoxicity can protect PBMC from infection by cell-associated HIV-1. *Clin. Immunol. 90:203.*
9. Poignard, P., R. Sabbe, G. R. Picchio, M. Wang, R. J. Gulizia, H. Katinger, P. W. Parren, D. E. Mosier, and D. R. Burton. 1999. Neutralizing antibodies have limited effects on the control of established HIV-1 infection in vivo. *Immunity 10:431.*
10. Rook, A. H., H. C. Lane, T. Folks, S. McCoy, H. Alter, and A. S. Fauci. 1987. Sera from HTLV-III/LAV antibody-positive individuals mediate antibody-dependent cellular cytotoxicity against HTLV-III/LAV-infected T cells. *J. Immunol. 138:1064.*
11. Ljunggren, K., V. Moschese, P. A. Broliden, C. Giaquinto, I. Quinti, E. M. Fenyo, B. Wahren, P. Rossi, and M. Jondal. 1990. Antibodies mediating cellular cytotoxicity and neutralization correlate with a better clinical stage in children born to human immunodeficiency virus-infected mothers. *J. Infect. Dis. 161:198.*
12. Evans, L. A., G. Thomson-Honnebier, K. Steimer, E. Paoletti, M. E. Perkus, H. Hollander, and J. A. Levy. 1989. Antibody-dependent cellular cytotoxicity is directed against both the gp120 and gp41 envelope proteins of HIV. *AIDS 3:273.*
13. Tyler, D. S., S. D. Stanley, S. Zolla-Pazner, M. K. Gorny, P. P. Shadduck, A. J. Langlois, T. J. Matthews, D. P. Bolognesi, T. J. Palker, and K. J. Weinhold. 1990. Identification of sites within gp41 that serve as targets for antibody-dependent cellular cytotoxicity by using human monoclonal antibodies. *J. Immunol. 145:3276.*
14. Rudensey, L. M., J. T. Kimata, E. M. Long, B. Chackerian, and J. Overbaugh. 1998. Changes in the extracellular envelope glycoprotein of variants that evolve during the course of simian immunodeficiency virus SIVMne infection affect neutralizing antibody recognition, syncytium formation, and macrophage tropism but not replication, cytopathicity, or CCR-5 coreceptor recognition. *J. Virol. 72:209.*
15. Alsmadi, O., and S. A. Tilley. 1998. Antibody-dependent cellular cytotoxicity directed against cells expressing human immunodeficiency virus type 1 envelope of primary or laboratory-adapted strains by human and chimpanzee monoclonal antibodies of different epitope specificities. *J. Virol. 72:286.*
16. Alsmadi, O., R. Herz, E. Murphy, A. Pinter, and S. A. Tilley. 1997. A novel antibody-dependent cellular cytotoxicity epitope in gp120 is identified by two monoclonal antibodies isolated from a long-term survivor of human immunodeficiency virus type 1 infection. *J. Virol. 71:925.*
17. Gomez-Roman, V. R., C. Cao, Y. Bai, H. Santamaria, G. Acero, K. Manoutcharian, D. B. Weiner, K. E. Ugen, and G. Gevorkian. 2002. Phage-displayed mimotopes recognizing a biologically active anti-HIV-1 gp120 murine monoclonal antibody. *J. Acquired Immune Defic. Syndr. 31:147.*
18. Ahmad, A., X. A. Yao, J. E. Tanner, E. Cohen, and J. Menezes. 1994. Surface expression of the HIV-1 envelope proteins in *env* gene-transfected CD4-positive human T cell clones: characterization and killing by an antibody-dependent cellular cytotoxic mechanism. *J. Acquired Immune Defic. Syndr. 7:789.*
19. Ahmad, R., S. T. Sindhu, E. Toma, R. Morisset, J. Vincelette, J. Menezes, and A. Ahmad. 2001. Evidence for a correlation between antibody-dependent cellular cytotoxicity-mediating anti-HIV-1 antibodies and prognostic predictors of HIV infection. *J. Clin. Immunol. 21:227.*
20. Ahmad, A., and J. Menezes. 1995. Positive correlation between the natural killer and gp 120/41-specific antibody-dependent cellular cytotoxic effector functions in HIV-infected individuals. *J. Acquir. Immune Defic. Syndr. Hum. Retrovirol. 10:115.*
21. Baum, L. L., K. J. Cassutt, K. Knigge, R. Khattri, J. Margolick, C. Rinaldo, C. A. Kleeberger, P. Nishanian, D. R. Henrard, and J. Phair. 1996. HIV-1 gp120-specific antibody-dependent cell-mediated cytotoxicity correlates with rate of disease progression. *J. Immunol. 157:2168.*
22. Hober, D., A. Jewett, and B. Bonavida. 1995. Lysis of uninfected HIV-1 gp120-coated peripheral blood-derived T lymphocytes by monocyte-mediated antibody-dependent cellular cytotoxicity. *FEMS Immunol. Med. Microbiol. 10:83.*
23. Lyerly, H. K., T. J. Matthews, A. J. Langlois, D. P. Bolognesi, and K. J. Weinhold. 1987. Human T-cell lymphotropic virus IIIB glycoprotein (gp120) bound to CD4 determinants on normal lymphocytes and expressed by infected cells serves as target for immune attack. *Proc. Natl. Acad. Sci. USA 84:4601.*
24. Watkins, B. A., S. Buge, K. Aldrich, A. E. Davis, J. Robinson, M. S. Reitz, Jr., and M. Robert-Guroff. 1996. Resistance of human immunodeficiency virus type 1 to neutralization by natural antisera occurs through single amino acid substitutions that cause changes in antibody binding at multiple sites. *J. Virol. 70:8431.*
25. Parren, P. W., M. Wang, A. Trkola, J. M. Binley, M. Purtscher, H. Katinger, J. P. Moore, and D. R. Burton. 1998. Antibody neutralization-resistant primary isolates of human immunodeficiency virus type 1. *J. Virol. 72:10270.*
26. Cheng-Mayer, C., A. Brown, J. Harouse, P. A. Luciw, and A. J. Mayer. 1999. Selection for neutralization resistance of the simian/human immunodeficiency virus SHIVSF33A variant in vivo by virtue of sequence changes in the extracellular envelope glycoprotein that modify *N*-linked glycosylation. *J. Virol. 73:5294.*
27. Ikuta, K., C. Morita, S. Miyake, T. Ito, M. Okabayashi, K. Sano, M. Nakai, K. Hirai, and S. Kato. 1989. Expression of human immunodeficiency virus type 1 (HIV-1) *gag* antigens on the surface of a cell line persistently infected with HIV-1 that highly expresses HIV-1 antigens. *Virology 170:408.*
28. Nishino, Y., K. Ohki, T. Kimura, S. Morikawa, T. Mikami, and K. Ikuta. 1992. Major core proteins, p24s, of human, simian, and feline immunodeficiency viruses are partly expressed on the surface of the virus-infected cells. *Vaccine 10:677.*
29. Koup, R. A., J. L. Sullivan, P. H. Levine, F. Brewster, A. Mahr, G. Mazzara, S. McKenzie, and D. Panicali. 1989. Antigenic specificity of antibody-dependent cell-mediated cytotoxicity directed against human immunodeficiency virus in antibody-positive sera. *J. Virol. 63:584.*
30. Hanna, Z., D. G. Kay, N. Rebai, A. Guimond, S. Jothy, and P. Jolicoeur. 1998. Nef harbors a major determinant of pathogenicity for an AIDS-like disease induced by HIV-1 in transgenic mice. *Cell 95:163.*
31. Kestler, H. W., III, D. J. Ringler, K. Mori, D. L. Panicali, P. K. Sehgal, M. D. Daniel, and R. C. Desrosiers. 1991. Importance of the *nef* gene for maintenance of high virus loads and for development of AIDS. *Cell 65:651.*
32. Miller, M. D., M. T. Warmerdam, I. Gaston, W. C. Greene, and M. B. Feinberg. 1994. The human immunodeficiency virus-1 *nef* gene product: a positive factor for viral infection and replication in primary lymphocytes and macrophages. *J. Exp. Med. 179:101.*
33. Jamieson, B. D., G. M. Aldrovandi, V. Planelles, J. B. Jowett, L. Gao, L. M. Bloch, I. S. Chen, and J. A. Zack. 1994. Requirement of human immunodeficiency virus type 1 *nef* for in vivo replication and pathogenicity. *J. Virol. 68:3478.*
34. Greenway, A. L., G. Holloway, and D. A. McPhee. 2000. HIV-1 Nef: a critical factor in viral-induced pathogenesis. *Adv. Pharmacol. 48:299.*
35. Varin, A., S. K. Manna, V. Quivy, A. Z. Decrion, C. Van Lint, G. Herbein, and B. B. Aggarwal. 2003. Exogenous nef protein activates NF-κB, AP-1 and c-Jun N-terminal kinase and stimulates HIV transcription in promonocytic cells: role in AIDS pathogenesis. *J. Biol. Chem. 273:2219.*
36. Fujii, Y., Y. Nishino, T. Nakaya, K. Tokunaga, and K. Ikuta. 1993. Expression of human immunodeficiency virus type 1 Nef antigen on the surface of acutely and persistently infected human T cells. *Vaccine 11:1240.*
37. Fujii, Y., K. Otake, Y. Fujita, N. Yamamoto, Y. Nagai, M. Tashiro, and A. Adachi. 1996. Clustered localization of oligomeric Nef protein of human immunodeficiency virus type 1 on the cell surface. *FEBS Lett. 395:257.*
38. Fujii, Y., K. Otake, M. Tashiro, and A. Adachi. 1996. Human immunodeficiency virus type 1 Nef protein on the cell surface is cytocidal for human $CD4^+$ T cells. *FEBS Lett. 393:105.*
39. Yamada, T., and A. Iwamoto. 1999. Expression of a novel Nef epitope on the surface of HIV type 1-infected cells. *AIDS Res. Hum. Retroviruses 15:1001.*
40. Yamada, T., and A. Iwamoto. 2000. Comparison of proviral accessory genes between long-term nonprogressors and progressors of human immunodeficiency virus type 1 infection. *Arch. Virol. 145:1021.*
41. Howell, D. N., P. E. Andreotti, J. R. Dawson, and P. Cresswell. 1985. Natural killing target antigens as inducers of interferon: studies with an immunoselected, natural killing-resistant human T lymphoblastoid cell line. *J. Immunol. 134:971.*

42. Yu, D., T. Shioda, A. Kato, M. K. Hasan, Y. Sakai, and Y. Nagai. 1997. Sendai virus-based expression of HIV-1 gp120: reinforcement by the V^- version. *Genes Cells 2:457.*
43. Yamada, T., N. Kaji, T. Odawara, J. Chiba, A. Iwamoto, and Y. Kitamura. 2003. Proline 78 is crucial for human immunodeficiency virus type 1 Nef to down-regulate class I human leukocyte antigen. *J. Virol. 77:1589.*
44. Lanier, L. L., A. M. Le, C. I. Civin, M. R. Loken, and J. H. Phillips. 1986. The relationship of CD16 (Leu-11) and Leu-19 (NKH-1) antigen expression on human peripheral blood NK cells and cytotoxic T lymphocytes. *J. Immunol. 136:4480.*
45. Collins, K. L., B. K. Chen, S. A. Kalams, B. D. Walker, and D. Baltimore. 1998. HIV-1 Nef protein protects infected primary cells against killing by cytotoxic T lymphocytes. *Nature 391:397.*
46. Collins, K. L., and D. Baltimore. 1999. HIV's evasion of the cellular immune response. *Immunol. Rev. 168:65.*
47. Cohen, G. B., R. T. Gandhi, D. M. Davis, O. Mandelboim, B. K. Chen, J. L. Strominger, and D. Baltimore. 1999. The selective down-regulation of class I major histocompatibility complex proteins by HIV-1 protects HIV-infected cells from NK cells. *Immunity 10:661.*
48. Yang, O. O., P. T. Nguyen, S. A. Kalams, T. Dorfman, H. G. Gottlinger, S. Stewart, I. S. Chen, S. Threlkeld, and B. D. Walker. 2002. Nef-mediated resistance of human immunodeficiency virus type 1 to antiviral cytotoxic T lymphocytes. *J. Virol. 76:1626.*
49. Bonaparte, M. I., and E. Barker. 2003. Inability of natural killer cells to destroy autologous HIV-infected T lymphocytes. *AIDS 17:487.*
50. Ojo-Amaize, E., P. G. Nishanian, D. F. Heitjan, A. Rezai, I. Esmail, E. Korns, R. Detels, J. Fahey, and J. V. Giorgi. 1989. Serum and effector-cell antibody-dependent cellular cytotoxicity (ADCC) activity remains high during human immunodeficiency virus (HIV) disease progression. *J. Clin. Immunol. 9:454.*
51. Dalgleish, A., A. Sinclair, M. Steel, D. Beatson, C. Ludlam, and J. Habeshaw. 1990. Failure of ADCC to predict HIV-associated disease progression or outcome in a haemophiliac cohort. *Clin. Exp. Immunol. 81:5.*
52. Mansour, I., C. Doinel, and P. Rouger. 1990. $CD16^+$ NK cells decrease in all stages of HIV infection through a selective depletion of the $CD16^+CD8^+CD3^-$ subset. *AIDS Res. Hum. Retroviruses 6:1451.*
53. Hu, P. F., L. E. Hultin, P. Hultin, M. A. Hausner, K. Hirji, A. Jewett, B. Bonavida, R. Detels, and J. V. Giorgi. 1995. Natural killer cell immunodeficiency in HIV disease is manifest by profoundly decreased numbers of $CD16^+CD56^+$ cells and expansion of a population of $CD16^{dim}CD56^-$ cells with low lytic activity. *J. Acquir. Immune Defic. Syndr. Hum. Retrovirol. 10:331.*
54. Watanabe, N., M. Tomizawa, A. Tachikawa-Kawana, M. Goto, A. Ajisawa, T. Nakamura, and A. Iwamoto. 2001. Quantitative and qualitative abnormalities in HIV-1-specific T cells. *AIDS 15:711.*
55. Andersson, J., S. Kinloch, A. Sonnerborg, J. Nilsson, T. E. Fehniger, A. L. Spetz, H. Behbahani, L. E. Goh, H. McDade, B. Gazzard, et al. 2002. Low levels of perforin expression in $CD8^+$ T lymphocyte granules in lymphoid tissue during acute human immunodeficiency virus type 1 infection. *J. Infect. Dis. 185:1355.*
56. Migueles, S. A., A. C. Laborico, W. L. Shupert, M. S. Sabbaghian, R. Rabin, C. W. Hallahan, D. Van Baarle, S. Kostense, F. Miedema, M. McLaughlin, et al. 2002. HIV-specific $CD8^+$ T cell proliferation is coupled to perforin expression and is maintained in nonprogressors. *Nat. Immun. 3:1061.*
57. Rukavina, D., G. Laskarin, G. Rubesa, N. Strbo, I. Bedenicki, D. Manestar, M. Glavas, S. E. Christmas, and E. R. Podack. 1998. Age-related decline of perforin expression in human cytotoxic T lymphocytes and natural killer cells. *Blood 92:2410.*

JOURNAL OF VIROLOGY, Aug. 2004, p. 8437–8445 Vol. 78, No. 16
0022-538X/04/$08.00+0 DOI: 10.1128/JVI.78.16.8437–8445.2004

Frequent Transmission of Cytotoxic-T-Lymphocyte Escape Mutants of Human Immunodeficiency Virus Type 1 in the Highly HLA-A24-Positive Japanese Population

Tae Furutsuki,[1,2]† Noriaki Hosoya,[1]† Ai Kawana-Tachikawa,[1]† Mariko Tomizawa,[1] Takashi Odawara,[3] Mieko Goto,[1] Yoshihiro Kitamura,[1] Tetsuya Nakamura,[3] Anthony D. Kelleher,[4] David A. Cooper,[4] and Aikichi Iwamoto[1,3]*

Division of Infectious Diseases, Advanced Clinical Research Center, Department of Infectious Diseases and Applied Immunology, Research Hospital,[1] and Institute of Medical Science,[3] University of Tokyo, Minato-ku, Tokyo 108-8639, and Department of Applied Biochemistry, Tokai University, Hiratsuka-shi, Kanagawa,[2] Japan, and National Centre in HIV Epidemiology and Clinical Research, University of New South Wales, Sydney, Australia[4]

Received 5 January 2004/Accepted 30 March 2004

Although Japan is classified as a country with a low prevalence of human immunodeficiency virus type 1 (HIV-1), domestic sexual transmission has been increasing steadily. Because 70% of the Japanese population expresses HLA-A24 (genotype HLA-A*2402), we wished to assess the effect of the dominant HLA type on the evolution and transmission of HIV-1 among the Japanese population. Twenty-three out of 25 A24-positive Japanese patients had a Y-to-F substitution at the second position [Nef138-10(2F)] in an immunodominant A24-restricted CTL epitope in their HIV-1 *nef* gene (Nef138-10). None of 12 A24-negative Japanese hemophiliacs but 9 out of 16 patients infected through unprotected sexual intercourse had Nef138-10(2F) ($P < 0.01$). Two of two A24-positive but none of six A24-negative Australians had Nef138-10(2F). Nef138-10(2F) peptides bound well to the HLA-A*2402 heavy chain; however, Nef138-10(2F) was expressed poorly on the cell surface from the native protein. Thus, HIV-1 with Nef138-10(2F) appears to be a cytotoxic-T-lymphocyte escape mutant and has been transmitted frequently by sexual contact among the highly A24-positive Japanese population.

While cytotoxic T lymphocytes (CTLs) exert immune pressure on human immunodeficiency virus type 1 (HIV-1) throughout the course of primary and chronic infection (4, 24, 30), HIV-1 escapes through a variety of immune evading mechanisms such as downregulation of HLA class I molecules by Nef (7, 32, 33, 36) and defects in differentiation and maturation of CTLs (2, 6, 27, 35). Viral mutation also plays a crucial role in immune escape, and CTL escape mutant viruses may appear early or late in the clinical course of infection (5, 14, 31). Mutations leading to CTL escape may occur at amino acid residues essential for major histocompatibility complex binding (8), for T-cell-receptor recognition (10), or in flanking regions that affect antigen processing (3, 26).

HIV-1 CTL escape mutants may be stable. One such example at the HLA-B27-restricted Gag epitope, which is related to slower disease progression in adults, could be transmitted vertically from mother to child (12). Although significant association between HLA alleles and polymorphism in reverse transcriptase sequences in a large cohort of patients indicated HIV-1 adaptation at a population level (28), direct horizontal transmission of CTL escape mutants is yet to be shown.

Japan is classified as a country of low HIV-1 prevalence; however, national HIV-1 and AIDS surveillance has shown a steady increase of HIV-1 and AIDS cases mainly through unprotected sexual intercourse (USI) (84% of HIV-1 patients and 71% of AIDS patients were infected through USI within the country) (1). The Japanese population is less polymorphic than other populations in that 70% express HLA-A24 (genotype HLA-A*2402) (13). We speculated that stable CTL escape mutants from HLA-A24 might be transmitted more frequently in Japan than in other countries where the prevalence of HLA-A24 is much lower. We postulated that Japanese hemophiliacs with HIV-1 infection might be a good comparator group since they were infected directly by contaminated blood products from abroad. We therefore examined an immunodominant CTL epitope in the *nef* gene (Nef138-10) in HLA-A24-positive and -negative hemophiliacs and compared the sequence with sequences from those patients infected through USI (13, 18). We included Caucasian Australians infected through USI as another control of transmission of CTL escape mutants in a country where HLA-A24 is less prevalent (19).

MATERIALS AND METHODS

Patient samples. For sequence analysis, blood specimens were collected in EDTA. Plasmas were separated and preserved at −80°C until use. For enzyme-linked immunospot (ELISPOT) assay, peripheral blood mononuclear cells (PBMCs) were separated from heparinized whole blood and used on the day of the assay. Patient HLA was typed serologically. In selected patients, HLA genotype was determined after written informed consent was obtained. The study was approved by institutional review boards. All patients serologically typed as A24 positive proved to be positive for HLA-A*2402.

RNA extraction and reverse transcription. Viral RNA was extracted from 140 μl of plasma from patients by using the QIAamp viral RNA Mini kit (QIAGEN) and subjected to reverse transcription according to the manufacturer's protocol with SuperScript II RNase H⁻ reverse transcriptase (Invitrogen) and 5 μM random primers (Takara).

* Corresponding author. Mailing address: Division of Infectious Diseases, Advanced Clinical Research Center, Institute of Medical Science, University of Tokyo, 4-6-1 Shirokanedai, Minato-ku, Tokyo 108-8639, Japan. Phone: 81-3-5449-5359. Fax: 81-3-54495427. E-mail: aikichi@ims.u-tokyo.ac.jp.

† T.F., N.H., and A.K.-T. contributed equally to this work.

PCR amplification and sequencing. Fifteen microliters of cDNA (a one-sixth volume of the reverse transcription reaction) was subjected to the first PCR. One-tenth of the first PCR was subjected to the nested PCR. PCR was performed by using Ex-Taq (Takara) with 35 cycles of 30 s at 94°C, 30 s at 58°C, 30 s at 72°C, and a final extension for 7 min at 72°C. The primer sets are as follows (all nucleotide positions are in accordance with the HIV-1 SF2 strain). For the *env* V3 region, first PCR primer set 1, primers CBE297P (5′-GGTAGAACAG ATGCATGAGGAT-3′) (consensus B *env*, nucleotides [nt] 297 to 318) and E7668 M (5′-TTCTCCAATTGTCCCTCATATCTCCTCCTCCA-3′) (SF2, nt 7668 to 7636) were used; and for the second PCR primer set 1, primers E6554P (5′-ATCAGTTTATGGGATCAAAGCC-3′) (SF2, nt 6554 to 6575) and E7353 M (5′-ACAATTTCTGGGTCCCCTCCTGAGGA-3′) (SF2, nt 7353 to 7328) were used. For the first PCR primer set 2, primers E6984P (5′-ACATGGAAT TAGGCCA-3′) (SF2, nt 6984 to 7000) and E7395 M (5′-TTACAGTAGAAA AATTCCCC-3′) (SF2, nt 7395 to 7375) were used; and for the second PCR primer set 2, primers E7028P (5′-GGCAGTCTAGCAGAAGAAGA-3′) (SF2, nt 7028 to 7047) and E7353 M (5′-ACAATTTCTGGGTCCCCTCCTGAGGA-3′) (SF2, nt 7353 to 7328) were used. For the first PCR primer set 3, primers P6951 (5′-GACCATGTACAAATGTCAGC-3′) (SF2, nt 6951 to 6970) and M7592 (5′-CTCTTGTTAATAGCAGCCCT-3′) (SF2, nt 7592 to 7573) were used; and for the second PCR primer set 3, primers E6984P (5′-ACATGGAA TTAGGCCA-3′) (SF2, nt 6984 to 7000) and E7353 M (5′-ACAATTTCTGGG TCCCCTCCTGAGGA-3′) (SF2, nt 7353 to 7328) were used.

For the Nef138-10 epitope, first PCR primer set 1, primers n226p (5′-CTCA GGTACCTTTAAGACCAATG-3′) (nt 9028 to 9050) and n650m (5′-GAAAG TCCCCAGCGGAAAGTCCC-3′) (nt 9474 to 9452) were used; and for the second PCR primer set 1, primers n296p (5′-GGGACTGGAAGGGCTAATT TGGT-3′) (nt 9098 to 9120) and n564m (5′-GAAATGCTAGTTTGCTGTCA AAC-3′) (nt 9387 to 9365) were used. For the first PCR primer set 2, primers P8923 (5′-TGGAAAAACATGGAGCAATCA-3′) (nt 8923 to 8944) and M9290 (5′-TCCTTCATTGGCCTCTTCTAC-3′) (nt 9290 to 9270) were used; and for the second PCR primer set 2, primers P8924 (5′-GGAAAAACATGGAGCAA TCAC-3′) (nt 8924 to 8945) and M9288 (5′-CTTCATTGGCCTCTTCTACCT-3′) (nt 9288 to 9268) were used. For the first PCR primer set 3, primers P8923 (5′-TGGAAAAACATGGAGCAATCA-3′) (nt 8923 to 8944) and n694m (5′-C AGCATCTGAGGGACGCCAC-3′) (nt 9525 to 9506) were used; and for the second PCR primer set 3, primers n226p (5′-CTCAGGTACCTTTAAGACCA ATG-3′) (nt 9028 to 9050) and n532m (5′-TCTCCGCGTCCTCCATCCCA-3′) (nt 9345 to 9326) were used.

The PCR products were electrophoresed through agarose gels and purified with a Minielute gel extraction kit (QIAGEN) before sequencing. Purified PCR products were directly sequenced. When sequence ambiguities resulted, DNA fragments were subcloned into the pGEM-T vector (Promega) and sequenced. DNA sequencing was performed by using an ABI Prism dye terminator cycle sequencing ready reaction kit (Applied Biosystems) on a Perkin-Elmer ABI-377 sequencer.

Cells and media. T2-A24, a kind gift from K. Kuzushima, was cultured in RPMI 1640 (Sigma) supplemented with 10% heat-inactivated fetal calf serum (FCS) (Sigma) and 0.8 mg of G418 (Invitrogen)/ml (25). We transformed PBMCs from an HLA-A*2402-positive person with human T-cell leukemia virus type 1 (HTLV-1) and established an HLA-A*2402- and CD4-positive-T-cell line (KWN-T4). KWN-T4 was cultured with RPMI 1640 supplemented with 25 U of interleukin-2 (Wako)/ml, 100 U of penicillin/ml, 100 U of streptomycin (Invitrogen)/ml, and 10% heat-inactivated FCS (JRH Bioscience). We also established Nef138-10-specific CTL clones as previously described (22). CTL clones were cultured with RPMI 1640 supplemented with 50 U of interleukin-2/ml, 100 U of penicillin/ml, 100 U of streptomycin/ml, and 10% heat-inactivated FCS.

Peptides. Synthetic peptides Nef138-10 (RYPLTFGWCF), 2F (RFPLTFGW CF), 5C (RYPLCFGWCF), and 2F5C (RFPLCFGWCF) were purchased from Sigma-Genosys. All peptides were more than 95% pure as determined by high-performance liquid chromatography and mass spectroscopy.

Peptide binding assays. Peptide binding to HLA-A*2402 was quantified by using a T2-A24 stabilization assay as previously described (25). T2-A24 cells were incubated at 26°C for 16 h, and then 2×10^5 cells were incubated with peptides at concentrations from 10^{-4} to 10^{-9} M for 1 h at 4°C. After incubation for 3 h at 37°C, the cells were stained with anti-HLA-A24 monoclonal antibody, A11.1 M (11), and an R-phycoerythrin (RPE)-conjugated $F(ab')_2$ fragment of anti-mouse immunoglobulin (DAKO). The mean fluorescence intensity was measured by FACSCalibur (Becton Dickinson).

ELISPOT assay and functional avidity analysis. Freshly prepared PBMCs (20,000 to 50,000) were added to 96-well multiscreen plates (Millipore) which had been precoated with 100 μl of 5 μg of anti-gamma interferon (IFN-γ) monoclonal antibody 1-D1K (Mabtech)/ml at room temperature for 3 h and blocked with RPMI 1640 medium containing 10% FCS for 1 h. The cells were cultured with synthetic peptide Nef138-10 or its derivatives at concentrations from 10^{-5} to 10^{-11} M for 18 h. After the plates were washed, 100 μl of 1 μg of biotinylated anti-IFN-γ monoclonal antibody 7-B6-1 (Mabtech)/ml was added and incubated at room temperature for 90 min. After the plates were washed again, 100 μl of 1:1,000-diluted streptavidin-alkaline phosphatase conjugate (Mabtech) was added and incubated at room temperature for 60 min. Spots were developed with an alkaline phosphatase conjugate substrate kit (Bio-Rad) and counted with a KS ELISPOT compact (Carl Zeiss). The IFN-γ responses to peptide dilutions were expressed as a percentage of the maximal IFN-γ response seen in each individual assay.

Expression of recombinant Nef protein. Mutations were introduced into *nef* derived from HIV-1 strain SF2 by site-directed mutagenesis based on overlap extension (16). Four proline residues in the Nef proline-rich domain that are important for HLA class I down-regulation were replaced by alanine as described previously (36). The wild type and various *nef* mutants were tagged by His_6 and introduced into a Sendai virus vector (SeV) as previously described (36). For Western blot analysis, KWN-T4 cells were infected with various SeVs at a multiplicity of infection of 10 and lysed 20 h after infection. Western blot analysis was performed according to the standard procedure. Anti-His_6 antibody (QIAGEN) and anti-SeV mouse antiserum were used to detect Nef and SeV proteins, respectively.

^{51}Cr release assay. Cytotoxicity was measured with a standard ^{51}Cr release assay as previously described (21). Briefly, KWN-T4 was labeled with 100 μCi of $Na_2^{51}CrO_4$ for 2 h and washed three times with R10. Labeled cells (2×10^3) were added to a 96-well round-bottom microtiter plate with a corresponding amount of peptide. After 1 h of incubation, Nef138-10-specific CTL clones were added and incubated for 4 h. When SeV-infected cells were used as target cells, the cells were infected with SeVs at a multiplicity of infection of 10, 20 h before adding the CTLs.

The supernatants were collected and analyzed with a microbeta counter. Spontaneous ^{51}Cr release was determined by measuring counts per minute in the supernatant of wells containing only target cells (cpm_{spn}). The maximum release (cpm_{max}) was determined by measuring the release of ^{51}Cr from target cells in the presence of 2% Triton X-100. Specific lysis was determined as follows: specific lysis = $(cpm_{exp} - cpm_{spn})/(cpm_{max} - cpm_{spn}) \times 100$, where cpm_{exp} represents the counts per minute in the supernatant of wells containing target and effector cells.

RESULTS

Sexual transmission of HIV-1 with stereotypic amino acid substitution among the Japanese population. Only patients infected with virus subtyped as B by phylogenic comparison of envelope sequences were included to avoid potential bias introduced by sequence differences across subtypes (data not shown). We extensively sequenced the Nef138-10 epitope and its flanking region from plasma HIV-1 RNA of 23 Japanese hemophiliacs (11 A24-positive and 12 A24-negative individuals) and 30 Japanese (14 A24-positive and 16 A24-negative individuals) and 8 Caucasian Australians (2 A24-positive and 6 A24-negative individuals) infected through USI (Table 1). Ten out of 11 A24-positive but none of A24-negative Japanese hemophiliacs had a Y-to-F amino acid substitution at the second position [Nef138-10(2F)] (Fig. 1A) ($P < 0.01$), suggesting that HLA-A24 selected for Nef138-10(2F). In the case of patients infected through USI, 13 out of 14 A24-positive and 9 out of 16 A24-negative Japanese patients had Nef138-10(2F) by direct sequencing (Fig. 1B) (data not significant). The frequency of Nef138-10(2F) was significantly higher in Japanese A24-negative patients infected through USI than A24-negative hemophiliacs ($P < 0.01$). Two out of two A24-positive but none of six A24-negative Caucasian Australians had Nef138-10(2F) (Fig. 1C). The frequency of Nef138-10(2F) in A24-negative patients infected through USI was significantly higher for Japanese patients than for Australian patients ($P < 0.05$), suggesting that sexual transmission of the variant was more

TABLE 1. Patient profile[a]

Patient ID	Sex	HLA type	No. of CD4 cells/μl	Viral load (copies/ml)	Sample date (mo/day/yr)	HIV subtype
A24-positive Japanese hemophiliacs						
A24-J037	M	A24/26, B35/51	207	180,000[b]	03/09/95	B
A24-J041	M	A24/26, B44/61	261	7,500[bd]	03/09/95	B
A24-J033	M	A24/26, B46/52	27	200,000[b]	03/27/95	B
A24-J035	M	A24, B40/48	148	360,000	04/10/95	B
A24-J031	M	A24/31, B51/60	29	180,000[b]	10/23/95	B
A24-J030	M	A11/24, B13/62	3	380,000[bd]	02/26/96	B
A24-J029	M	A24/31, B35/61	38	ND	04/01/96	B
A24-J036	M	A2 /24, B35/51	60	74,000[b]	05/13/96	B
A24-J034	M	A24, B46/52	180	74,000[bd]	05/20/96	B
A24-J038	M	A2 /24, B51/62	356	29,000[b]	03/03/97	B
A24-J005	M	A24, B52/70	39	220,000[b]	06/19/97	B
A24-negative Japanese hemophiliacs						
NA24-J037	M	A26, B40	8	>1,600,000[bd]	06/08/95	B
NA24-J035	M	A11/26, B54/56	342	100,000[b]	09/07/95	B
NA24-J031	M	A2/26, B51/61	521	130,000[b]	09/18/95	B
NA24-J041	M	A26, B39/54	12	700,000[bd]	10/05/95	B
NA24-J032	M	A2/11, B46/54	1[d]	150,000[b]	11/10/95	ND
NA24-J030	M	A31/33, B44/51	363	65,000[b]	03/21/96	B
NA24-J040	M	A2/33, B17/54	101	74,000[b]	03/21/96	ND
NA24-J033	M	A26, B61	143	140,000[b]	04/18/96	B
NA24-J029	M	A11/33, B44/51	401	<10,000	07/15/96	B
NA24-J034	M	A11/33, B17/56	38	81,000[b]	08/15/96	B
NA24-J039	M	A11/26, B51/62	3	88,000[b]	09/01/97	B
NA24-J006	M	A2/26, B39/61	335	9,200	10/30/00	B
A24-positive Japanese infected through USI						
A24-J006	M	A2/24, B7/54	212	33,000	09/19/97	B
A24-J007	M	A24/26, B17/56	103	120,000	11/06/97	B
A24-J009	M	A24, B48/52	278	4,500	01/19/98	B
A24-J010	M	A24, B52	393	18,000	03/09/98	B
A24-J024	M	A24, B35/61	274	110,000	10/27/98	B
A24-J012	M	A24/26, B46/60	253	24,000	07/19/99	B
A24-J013	M	A24/26, B35/48	168	15,000	9/20/99	B
A24-J016	M	A11/24, B7/55	245	150,000	05/15/00	B
A24-J017	M	A1/24, B54/70	255	70,000	10/17/00	B
A24-J018	M	A24/31, B37/61	185	8,300	01/04/01	B
A24-J025	M	A24, B51/52	282	130,000	06/07/01	B
A24-J023	M	A2/24, B51/54	856[d]	17,000[d]	08/06/01	B
A24-J021	M	A2/24, B46/52	344	35,000	11/26/01	B
A24-J026	M	A2/24, B13/51	381	110,000	11/28/01	B
A24-negative Japanese infected through USI						
NA24-J025	M	A2/31, B51/61	352	18,000[b]	03/23/95	B
NA24-J023	M	A11/26, B35/51	23	5,000[b]	04/01/96	ND
NA24-J021	M	A26, B52/54	9	44,000	08/04/97	B
NA24-J018	M	A2, B39/60	378	72,000	04/06/98	B
NA24-J017	M	A11/31, B51/56	197	72,000	04/16/98	B
NA24-J016	M	A3/31, B51/58	257	200,000	05/25/98	B
NA24-J015	M	A2/26, B51/62	543	13,000	06/26/98	B
NA24-J012	M	A31, B13/51	268	26,000	10/19/98	B
NA24-J011	M	A2, B55/60	408	12,000	10/22/98	B
NA24-J010	M	A2/26, B51/61	206	16,000	12/17/98	B
NA24-J009	M	A2, B52/60	115	850,000	05/24/99	B
NA24-J008	M	A11/33, B44/60	312	2,600	07/08/99	ND
NA24-J007	M	A26, B7/52	396	450	08/09/00	B
NA24-J005	M	A2/31, B48/52	604	17,000	01/18/01	B
NA24-J003	M	A31/33, B44/51	308	20,000	06/04/01	B
NA24-J002	M	A2/33, B44/46	496	14,000	09/27/01	ND
A24 positive Australian infected through USI						
A24-A001	M	A3/24, B7	255	38,000	08/16/96	ND
A24-A002	M	A24/30, B13	598	21,700	03/22/01	B
A24-negative Australian infected through USI						
NA24-A007	M	A2/3, B7	704	ND[c]	11/02/95	B
NA24-A005	M	A1/3, B8/70	620	7,700	05/26/96	B
NA24-A013	M	A32, B13/64	851	23,200	09/28/98	B
NA24-A008	M	A2/3, B39/44	543	52,836	01/04/99	B
NA24-A003	M	A2, B18/62	575	19,400	11/06/99	B
NA24-A006	M	A3/26, B18/27	594	18,200	04/13/00	B

[a] ND, not determined.
[b] Data were obtained by Branch DNATM version 1.0.
[c] Nearest data were 17,000 with CD4 counts of 638.
[d] Nearest data were within 6 months of sample collection.

A

A24-positive Japanese hemophiliacs

Patient ID	flanking WQNYTPGPGI	CTL epitope RYPLTFGWCF	flanking KLVPVEPEKV
A24-J041	---------V	-F--------	---------M
A24-J033	-----E---T	-F-------Y	-------D--
A24-J031	-H-------T	-F--------	-
A24-J030	---------T	-F--C-----	----------
A24-J034	---------T	-F--------	-----DQ-Q-
A24-J038	---------	----C-----	-----D-D--
A24-J005	-D/E-------T	-F--------	-
A24-J029	---------V/T	-F--------	--------Q-
A24-J037	--C------T	-F--------	-----D----
A24-J035	---------T	-F--------	----------
A24-J036	--C------T	-F--------	----------

A24-negative Japanese hemophiliacs

Patient ID	flanking WQNYTPGPGI	CTL epitope RYPLTFGWCF	flanking KLVPVEPEKV
NA24-J037	----------	----------	----------
NA24-J035	----------	----------	----M-----
NA24-J031	----------	----------	-------G/E-V/I
NA24-J041	----------	----------	--------DE
NA24-J032	----------	----------	----M-----
NA24-J030	--S------V	----C-----	----------
NA24-J040	----------	----------	---------I
NA24-J033	----------	----------	-L/V--------
NA24-J029	-H--------	----------	--------D-
NA24-J034	----------	----------	----V/L-----
NA24-J039	----------	----C-----	-----D-D--
NA24-J006	---------V	----C-----	-----D----

B

A24-positive Japanese infected through USI

Patient ID	flanking WQNYTPGPGI	CTL epitope RYPLTFGWCF	flanking KLVPVEPEKV
A24-J006	---------V	-F--------	-----E/D--Q-
A24-J007	---------T	-F--C-----	----A---E-
A24-J009	---------T	-F--------	-
A24-J010	---------T	-F--------	-------QR-
A24-J012	---------T	-F--------	-------D--
A24-J013	---------T	-F--------	-----D-DQ-
A24-J016	-D-------V	----C-----	-----DQD--
A24-J017	-D-------T	-F--C-----	---------I
A24-J018	---------T	-F--------	---------I
A24-J023	---------T	-F--------	----L--GEA
A24-J021	---------T	-F--------	-----D-DQ-
A24-J024	---------T	-F--------	-----D-D--
A24-J025	-D-------T	-F--------	-----DQDQ-
A24-J026	---------T	-F--------	-------KQ-

A24-negative Japanese infected through USI

Patient ID	flanking WQNYTPGPGI	CTL epitope RYPLTFGWCF	flanking KLVPVEPEKV	
NA24-J025	-H-------V	----C-----	-----D-D/AQ-	
NA24-J023*	---------T	-Y/W/F--------	---------I	Y 2/11,F 3/11,W 5/11
NA24-J021	----------	----------	-----N--Q-	
NA24-J018*	---------T	-Y/F--C-----	----------	Y 8/10,F 2/10
NA24-J017*	---------T	-Y/F--------	----L-----	Y 5/13,F 8/13
NA24-J016	---------V	----------	----L---Q-	
NA24-J015	---------T	-F--------	-----D-DQ-	
NA24-J012	-H/QS------T	----------	-----D-DQ-	
NA24-J011	---------T	-F--------	-------NQ-	
NA24-J010	-	----------	-	
NA24-J009	---------T	-F--------	-------NQ-	
NA24-J008	-D-------T	-F--------	----L---Q-	
NA24-J007	---------T	-F--------	-------NQ-	
NA24-J005	-G/D-------T	-F--------	-----DQDQ-	
NA24-J003	-H--------	----------	-----DQ---	
NA24-J002	-Q/HG-------	----------	-----D-DQ-	

C

A24-positive Australian infected through USI

Patient ID	flanking WQNYTPGPGI	CTL epitope RYPLTFGWCF	flanking KLVPVEPEKV
A24-A001	---------T	-F--------	----------
A24-A002	---------T	-F--------	----M-----

A24-negative Australian infected through USI

Patient ID	flanking WQNYTPGPGI	CTL epitope RYPLTFGWCF	flanking KLVPVEPEKV
NA24-A007	---------V	----------	-
NA24-A005	---------V	----------	----------
NA24-A013	----------	----------	----------
NA24-A008	-H--------	----------	----M-P/Q---
NA24-A003	-H--------	----------	-----D-D--
NA24-A006	----------	----C-----	--------E-

FIG. 1. Nef138-10 epitope and its flanking sequences. Amino acid sequences deduced from the direct DNA sequencing of Nef138-10 CTL epitope and both flanking regions are presented. Wild-type sequences (HIV-1 strain SF2) are presented on the top. Dashes indicate the same amino acid as that of the wild type. Sequence substitutions are presented by single amino acid characters. Where a mixture of two or three amino acids was plausible, two or three amino acids were shown together separated by a shill. A single dash indicates that the sequences could not be determined by ambiguities. (A) Sequences from A24-positive and -negative Japanese hemophiliacs. (B) Sequences from A24-positive and -negative Japanese patients infected through USI. Asterisks indicate samples for which sequence ambiguities were found by direct sequence analysis. We cloned these PCR fragments into the pGEM-T vector and sequenced each 10 to 13 colonies. All amino acid sequences are indicated. (C) Sequences from A24-positive and -negative Australians infected through USI.

frequent among the Japanese population, which has a higher prevalence of HLA-A*2402.

Nef138-10(2F) accompanied a particular amino acid substitution in the N-terminal flanking region. We detected an I-to-T substitution at the −1 position (−1T) in 32 flanking sequences out of 34 accompanying Nef138-10(2F) sequences (94%), while others were two I-to-V substitutions (Fig. 1). The −1T substitution was quite unusual in the flanking region of the wild-type Nef138-10 CTL epitope in our cohort (Fig. 1).

Reversion of CTL escape mutants. Since three acutely infected A24-positive patients (A24-J023, A24-J024, and A24-J025) had Nef138-10(2F) in their earliest plasma samples available, we could not demonstrate the evolution of Nef138-10(2F) from the wild type under the selective pressure of HLA-A*2402 (data not shown). However, we could analyze serial samples from chronically infected A24-negative patients who had been followed without treatment over years. All the 12 cloned sequences in the earliest plasma samples available from NA24-J015 had F at the second position; however, 11 out of 11 clones displayed wild-type sequence within a year (Fig. 2A). It is interesting that the −1T substitution in the flanking region was present for at least a further two years before reverting to the wild type (Fig. 2A). In another chronically infected A24-negative patient (NA24-J018), we observed that the proportion of Nef138-10(2F) decreased gradually but persisted in the plasma for almost two years after the start of the follow-up (Fig. 2B). This patient had a T-to-C substitution at the fifth position with [Nef138-10(2F5C)] or without [Nef138-10(5C)] a substitution at the second position (Fig. 2B). Interestingly, the ratio of Nef138-10(2F5C) to Nef138-10(5C) decreased as time went by (Fig. 2B), suggesting that Nef138-10(5C) is more stable than Nef138-10(2F5C). Actually, we observed Nef138-10(5C) in both A24-positive and -negative patients (Fig. 1).

In order to elucidate the higher stability of the 5C rather than the 2F substitution, we examined the codon usage at these positions (data not shown). The wild-type codon for the second tyrosine (Y) residue in Nef138-10 was coded by TAT or TAC in 23 (77%) and 12 (40%) out of 30 patients, respectively. Five patients (17%) had a mixture of TAT and TAC for the codon (data not shown). Mutated nucleotide triplet TTT or TTC was responsible for the Y-to-F amino acid substitution in 27 (80%) and 9 (26%) out of 34 patients, respectively (data not shown).

A

	Sample Date	nef138-10			
Patient ID	M/D/Y	WQNYTPGPGI	RYPLTFGWCF	KLVPVEPEKV	cloning
NA24-J015	06/26/98	---------T	-F--------	-----D-DQ-	direct
		---------T	-F--------	-----D-DQ-	11/12
		---------T	-F-----R--	-----D-DQ-	1/12
NA24-J015	06/07/99	---------T	-Y--------	-----D-DQ-	direct
		---------T	-Y--------	-----D-DQ-	9/11
		-R-------T	-Y--------	-----D-DQ-	1/11
		---------T	-Y--------	--I--D-DQ-	1/11
NA24-J015	03/09/00	---------T	-Y--------	-----D-DQ-	direct
NA24-J015	04/16/01	---------T	-Y--------	-----D-DQ-	direct
NA24-J015	01/16/03	----------	-Y--------	-----D-DQ-	direct
		----------	-Y--------	-----D-DQ-	10/10

B

	Sample Date	nef138-10			
Patient ID	M/D/Y	WQNYTPGPGI	RYPLTFGWCF	KLVPVEPEKV	cloning
NA24-J018	04/08/96	---------T	-F--C-----	--------Q-	direct
		---------T	-F--C-----	--------Q-	7/11
		---------P	-F--C-----	--------Q-	3/11
		---------P	-Y--C-----	--------Q-	1/11
NA24-J018	06/02/97	---------T	-F/Y--C-----	--------Q-	direct
		---------T	-F--C-----	--------Q-	7/13
		---------T	-Y--C-----	--------Q-	3/13
		---------A	-Y--C-----	--------Q-	1/13
NA24-J018	04/06/98	---------T	-Y/F--C-----	----------	direct
		---------T	-Y--C-----	--------Q-	6/10
		---------T	-F--C-----	--------Q-	2/10
		---------T	-Y--C-----	----------	2/10

FIG. 2. Serial Nef138-10 epitope and its flanking sequences in two A24-negative patients. Data are shown as described in the legend to Fig. 1. Fractional numbers in the right-most column indicate clone numbers with the sequences shown in the numerator and total clone numbers sequenced shown in denominator. "Direct" indicates the result of direct sequencing. (A) Patient NA24-Jo15. (B) Patient NA24-J018.

In two patients (6%) Nef138-10(2F) was coded by a mixture of HIV-1 using TTT and TTC for the codon. It appeared that at least one point mutation was necessary for the Y-to-F amino acid substitution. The wild-type codon for the fifth threonine (T) residue in Nef138-10 was coded by ACC or ACT in 49 (98%) and 2 (4%) out of 50 patients. One patient (2%) had a mixture of ACC and ACT. Mutated nucleotide triplet TGC or TGT was responsible for the T-to-C amino acid substitution in 5 (45%) and 6 (55%) out of 11 patients, respectively (data not shown). It appeared that at least two nucleotides had to be mutated for the T-to-C amino acid substitution, although we could not exclude the possibility of a three-nucleotide mutation for the amino acid substitution. Therefore, a Y-to-F amino acid substitution, or vice versa, at the second position required less nucleotide mutations than did the T-to-C substitution at the fifth position.

Peptide-based analysis of Nef138-10 and its variants. We measured the binding affinities of Nef138-10 and its variants to HLA-A*2402 (Fig. 3). Although a Y-to-F substitution occurred at the amino acid crucial for peptide affinity with the binding groove, Nef138-10(2F) binding to the HLA-A*2402 heavy chain was essentially preserved. However, the acquisition of a T-to-C substitution at the fifth position, such as Nef138-10(2F5C) and Nef138-10(5C), greatly reduced the binding affinity (Fig. 3). A functional avidity assay in which PBMCs from five patients were used confirmed the results of the binding assay (Fig. 4). Namely, the patients' PBMCs recognized Nef138-10(2F) at a very low concentration (one-half maximum response <1 nM) and had equivalent or even higher functional avidity than did the wild-type peptide. On the contrary, patients' PBMCs showed very low functional avidity against Nef138-10(2F5C) and Nef138-10(5C) (one-half maximum response >100 nM).

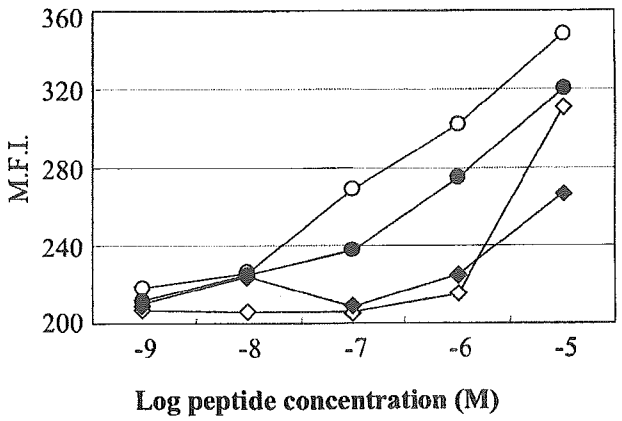

FIG. 3. Binding of the wild-type and mutant peptides to HLA*2402 molecules. Peptide binding to HLA-A*2402 was quantified by using a T2-A24 stabilization assay. Symbols: ○, wild type; ●, 2F; ◇, 5C; ◆, 2F5C. M.F.I., mean fluorescence intensity.

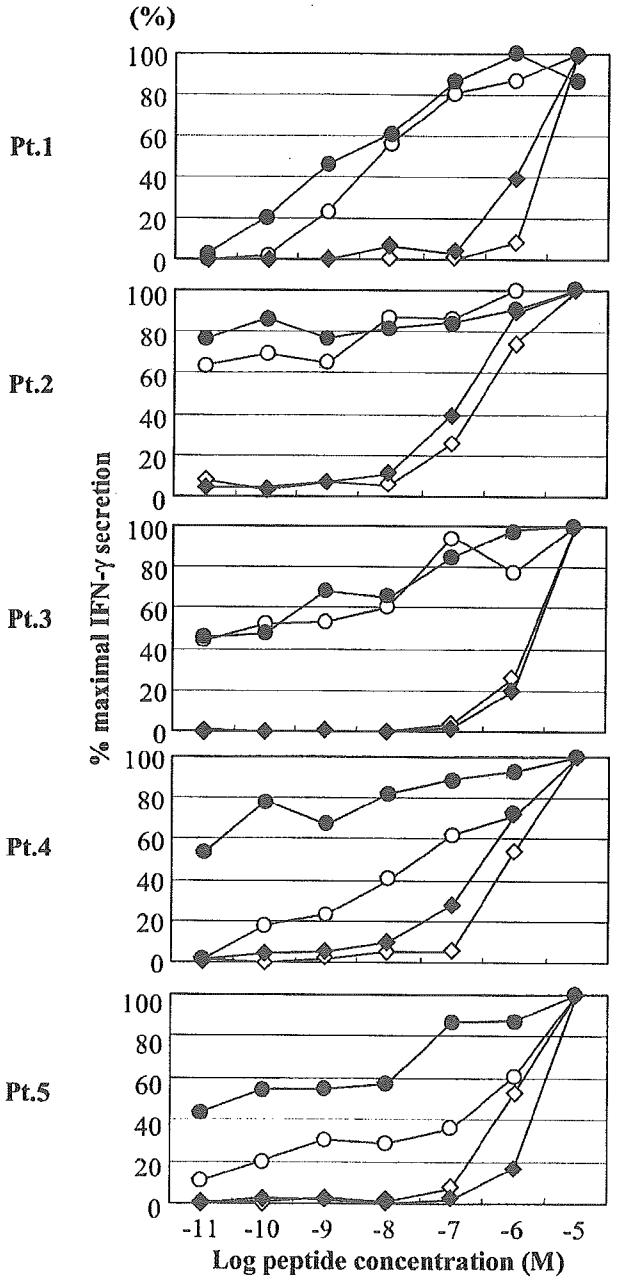

FIG. 4. Functional avidity assay. The reactivity of peptide-specific cells in PBMCs from five patients against log-fold dilutions of peptide was determined. Symbols: ○, wild type. ●, 2F; △, 5C; ◆, 2F5C.

Epitope presentation from native Nef protein. Strong selection for Nef138-10(2F) in the presence of CTLs with high in vivo functional avidity against the peptide prompted us to examine the processing and presentation of the Nef138-10 CTL epitope from the native protein. Native Nef proteins containing wild-type or variant CTL epitopes were expressed in an HLA-A*2402-positive-T-cell line (KWN-T4) via SeV. CTL epitope presentation was examined by two CTL clones established from A24-positive patients outside these cohorts. Although the two CTL clones were established by stimulation with the wild-type peptide (Nef138-10), they killed the target cells pulsed with Nef138-10(2F) peptides almost as well as the wild type (Fig. 5A and B). Both CTL clones efficiently killed the target cells expressing either wild-type Nef or Nef with −1T substitution in the flanking region (−1T2Y5T). However, these CTL clones failed to kill the target cells infected with vectors expressing Nef138-10(2F) with (−1T2F5T) or without (−1I2F5T) the −1T substitution in the flanking region. As expected, the CTL clones did not kill the target cells infected with a vector coding Nef138-10(2F5C), a nonbinding mutant (−1I2F5C) (Fig. 5A and B). Western blot analysis revealed that Nef proteins with wild-type or variant CTL epitopes were expressed abundantly in the target cells. Taken together, these data indicate that a Y-to-F substitution within the CTL epitope itself but not the −1T substitution in the flanking region resulted in the poor antigen presentation against CTL, which resulted in the escape.

DISCUSSION

We showed a significantly higher prevalence of a stereotypic amino acid substitution [Nef138-10(2F)] at an A24-restricted CTL epitope in Nef among A24-positive Japanese hemophiliacs compared with A24-negative counterparts. The origin of their HIV-1 infection was from the plasma collected and processed in Western countries where HLA-A*2402 was less prevalent (19). It is inferred that Nef138-10(2F) might be rare in a population where HLA-A*2402 is not prevalent but that it has a selective advantage in the presence of HLA-A*2402. Our findings with Australians are consistent with this notion. Although we examined only two HIV-1-infected A24-positive Caucasian Australians, both had Nef138-10(2F). On the other hand, Nef138-10(2F) was rare in A24-negative Australians. Japanese and Australians are distinctly different in the frequency of HLA-A*2402 within their respective populations (allele frequency of HLA-A24 is 35.1 and 7.8%, respectively) (19). Nef138-10(2F) was also positively selected among Japanese patients who were infected through USI. Interestingly, we detected Nef138-10(2F) frequently among A24-negative Japanese who were infected through USI. The result suggests that HIV-1 that went through selective pressure by HLA-A*2402 is actually circulating among the Japanese population because of the high prevalence of HLA-A24. Although we showed the reversion of Nef138-10(2F) to the wild type, it occurred very slowly over years, allowing the horizontal spread via sexual contact. In this study, we showed that HIV-1 with Nef138-10(2F) is actually a CTL escape mutant. Although the stereotypic Y-to-F substitution occurred at an anchor residue, Nef138-10(2F) peptide did bind to HLA-A*2402 heavy chain with almost the same efficiency as did the wild type (Fig. 3). This result is consistent with the algorithm prediction of the published binding motif (http://hiv-web.lanl.gov/content/immunology/motif_scan/motif.html). When native Nef proteins with or without a substitution were overexpressed in the A24-positive target cells via SeV, the Y-to-F substitution at the second position of the CTL epitope virtually abolished the killing by the CTL clones. The substitution in the flanking region did not affect the killing substantially. Therefore, the mechanism for the CTL escape appeared to reside in the processing of native Nef proteins and subsequent antigen presentation rather than HLA binding. A proteosomal cleavage